ADVANCED MATERIALS
www.advmat.de

Optoelectronic Properties of Single-Wall Carbon Nanotubes

*Sébastien Nanot, Erik H. Hároz, Ji-Hee Kim, Robert H. Hauge, and Junichiro Kono**

Single-wall carbon nanotubes (SWCNTs), with their uniquely simple crystal structures and chirality-dependent electronic and vibrational states, provide an ideal laboratory for the exploration of novel 1D physics, as well as quantum engineered architectures for applications in optoelectronics. This article provides an overview of recent progress in optical studies of SWCNTs. In particular, recent progress in post-growth separation methods allows different species of SWCNTs to be sorted out in bulk quantities according to their diameters, chiralities, and electronic types, enabling studies of (*n*,*m*)-dependent properties using standard macroscopic characterization measurements. Here, a review is presented of recent optical studies of samples enriched in 'armchair' (*n* = *m*) species, which are truly metallic nanotubes but show excitonic interband absorption. Furthermore, it is shown that intense ultrashort optical pulses can induce ultrafast bandgap oscillations in SWCNTs, via the generation of coherent phonons, which in turn modulate the transmission of a delayed probe pulse. Combined with pulse-shaping techniques, coherent phonon spectroscopy provides a powerful method for studying exciton-phonon coupling in SWCNTs in a chirality-selective manner. Finally, some of the basic properties of highly aligned SWCNT films are highlighted, which are particularly well-suited for optoelectronic applications including terahertz polarizers with nearly perfect extinction ratios and broadband photodetectors.

1. Introduction

Single-wall carbon nanotubes (SWCNTs)[1,2] represent one of the most direct realizations of a one-dimensional (1D) electron system available for fundamental studies today, attracting much theoretical interest.[3–14] At the same time, they are one of the leading candidates to replace conventional semiconductors in future optoelectronics, unifying electronic and photonic functions in nanoscale circuits.[15–17] Their unique physical, chemical, and mechanical properties have been extensively studied for the last two decades and reviewed elsewhere.[18–22]

During the past decade, much progress has been made in the study of optical and optoelectronic properties of SWCNTs, initiated by the 2002 discovery of bandgap photoluminescence (PL) from individually suspended SWCNTs in aqueous solutions at Rice University.[23] Such samples have opened up possibilities to perform spectroscopy of individual nanotubes of specific chiralities, instigating a flurry of optical spectroscopic studies with stimulating results: PL excitation (PLE) spectroscopy,[24–35] resonant Raman scattering (RRS) spectroscopy,[36–58] ultrafast optical spectroscopy,[59–90] micro- and nanospectroscopy,[91–113] and magneto-optical spectroscopy[106,107,114–124] of individualized SWCNTs are currently under intense investigation, revealing some fundamental properties of 1D excitons and phonons. In addition, many groups have investigated the photoconductivity of various SWCNT device structures to assess their properties as photodetectors and solar cells.[91,98,100,102,109,125–154]

There have been many theoretical studies on the electronic, optical, and magnetic properties of SWCNTs,[3,155–186] some of them preceding the discovery of this exotic 1D system in 1993. SWCNTs can be either semiconducting or metallic, depending on their geometrical characteristics (chiral angle). Their structure can be specified by a pair of integers (*n*,*m*) describing the chiral vector $\vec{C}_h = n\vec{a}_1 + m\vec{a}_2$, which connects two crystallographically equivalent sites on a 2D graphene sheet.[18–22] The general rules are: i) (*n*,*n*) tubes ("armchair" tubes) are metals; ii) (*n*,*m*) tubes with $n - m = 3j$ (*j*: nonzero integer) are small-gap (≈1–100 meV) semiconductors; and iii) all others are medium-gap (≈0.5–1 eV) semiconductors. The (*n*,*m*) indices of nanotubes in categories i) and ii) satisfy $\nu \equiv (n - m) \bmod 3 = 0$, whereas, for nanotubes in category iii), $\nu = \pm 1$. Schematic dispersion relations and corresponding densities of states of: a) armchair ($n = m$) and b) semiconducting ($\nu = \pm 1$) nanotubes are shown in **Figure 1**. It should be emphasized that, while armchair ($n = m$) nanotubes are metallic (gapless), nonarmchair (or $n \neq m$) $\nu = 0$ tubes have small curvature-induced bandgaps (i.e., they are, in fact, narrow-gap semiconductors).[3,158]

SWCNTs come in different types, and raw product is generally a mixture of numerous chiral configurations. Electron

Dr. S. Nanot, E. H. Hároz, Dr. J.-H. Kim, Prof. J. Kono
Department of Electrical and Computer Engineering
Department of Physics and Astronomy
The Richard E. Smalley Institute for
Nanoscale Science and Technology
Rice University
Houston, Texas, 77005, USA
E-mail: kono@rice.edu
Dr. R. H. Hauge
The Richard E. Smalley Institute for
Nanoscale Science and Technology
Department of Chemistry
Rice University
Houston, Texas, 77005, USA

DOI: 10.1002/adma.201201751

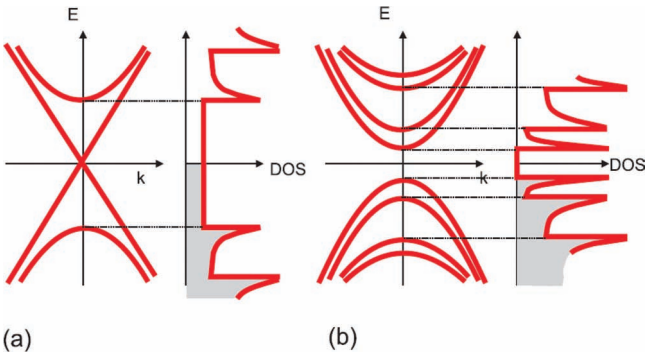

Figure 1. Schematic electronic energy-dispersion relations and densities of states of: a) metallic ($n = m$) and b) semiconducting ($\nu = \pm 1$) single-wall carbon nanotubes.

diffraction is a powerful technique for the determination of atomic structure of individual nano-objects, as was demonstrated in Iijima's original work on multiwall[187] and single-wall[1] carbon nanotubes. However, it is not suited for studying a large number of carbon nanotubes. Therefore, optical spectroscopy has emerged in the last decade as the most convenient means for determining the chirality indices (n,m) of SWCNTs in macroscopic ensembles of SWCNTs. There is now a well-established correlation between optical transition energies, diameters, and (n,m) indices, as shown in **Figure 2**a.[188] RRS spectroscopy has served as the most commonly used tool for (n,m) determination for both metallic and semiconducting SWCNTs for many years.[189] For semiconducting, or $\nu = \pm 1$, SWCNTs, PLE spectroscopy[24–35] can provide accurate information on the E_{11} and E_{22} energies from the emission and excitation photon energies, respectively, as shown in Figure 2b. One can also combine PLE and RRS spectroscopies to determine E_{33} and E_{44} in semiconducting nanotubes.[190] Furthermore, as detailed in Section 3, coherent phonon spectroscopy has several advantages for simultaneously determining (n,m) indices and phonon frequencies for both semiconducting and metallic SWCNTs (see Figure 2c). Finally, Section 4 presents how aligned SWCNT films can be used to develop optoelectronic devices, ranging from state-of-the-art terahertz polarizers to large-area, broadband photodetectors.

2. Enrichment and Spectroscopy of Armchair Carbon Nanotubes

Because of their excellent electrical properties, metallic SWCNTs are considered to be promising candidates for a variety of future electronic applications such as nanocircuit interconnects and power transmission cables. In particular, (n,n)-chirality, or 'armchair,' metallic nanotubes are theoretically predicted to be truly gapless and intrinsically insensitive to disorder,[191–192] consistent with experimentally observed ballistic conduction behavior at the single-tube level. Unfortunately, progress towards creating such ballistic-conducting armchair devices in bulk quantities has been slowed by the inherent problem of nanotube synthesis, whereby both semiconducting and metallic nanotubes are produced.

Sébastien Nanot received his Ph.D. from Université de Toulouse (France) in 2009 under supervision by Profs. Bertrand Raquet and Jean-Marc Broto. His thesis focused on individual carbon nanotube properties under a very high magnetic field. He moved to Rice University where he is appointed as a postdoctoral researcher in Prof. Junichiro Kono's group. His current research focuses on optoelectronic properties of carbon nanotubes ensembles.

Junichiro Kono received his B.S. and M.S. degrees in applied physics from the University of Tokyo in 1990 and 1992, respectively, and his Ph.D. in physics from the State University of New York at Buffalo in 1995. He was a postdoctoral researcher at the University of California, Santa Barbara in 1995–1997 and the W. W. Hansen Experimental Physics Laboratory Fellow at Stanford University in 1997–2000. He joined Rice University in 2000 as an Assistant Professor and was promoted to Associate Professor in 2005. Since 2009, he has been a Professor of Electrical & Computer Engineering and Physics & Astronomy.

Ji-Hee Kim received her B.S., M.S. and Ph.D. in physics from Chungnam National University (Republic of Korea) in 2005, 2007, and 2011, respectively, under supervision by Prof. Ki-Ju Yee. Her thesis focused on coherent optical phonons in graphene and single-wall carbon nanotubes via ultrafast spectroscopy. She moved to Rice University as a postdoctoral researcher in Prof. Junichiro Kono's group. Her current research focuses on many-body processes of excitons in quantum wells under high magnetic fields.

Recent years have seen impressive progress in separating SWCNTs by type, diameter, and chirality. One of the most successful methods is the technique of density gradient

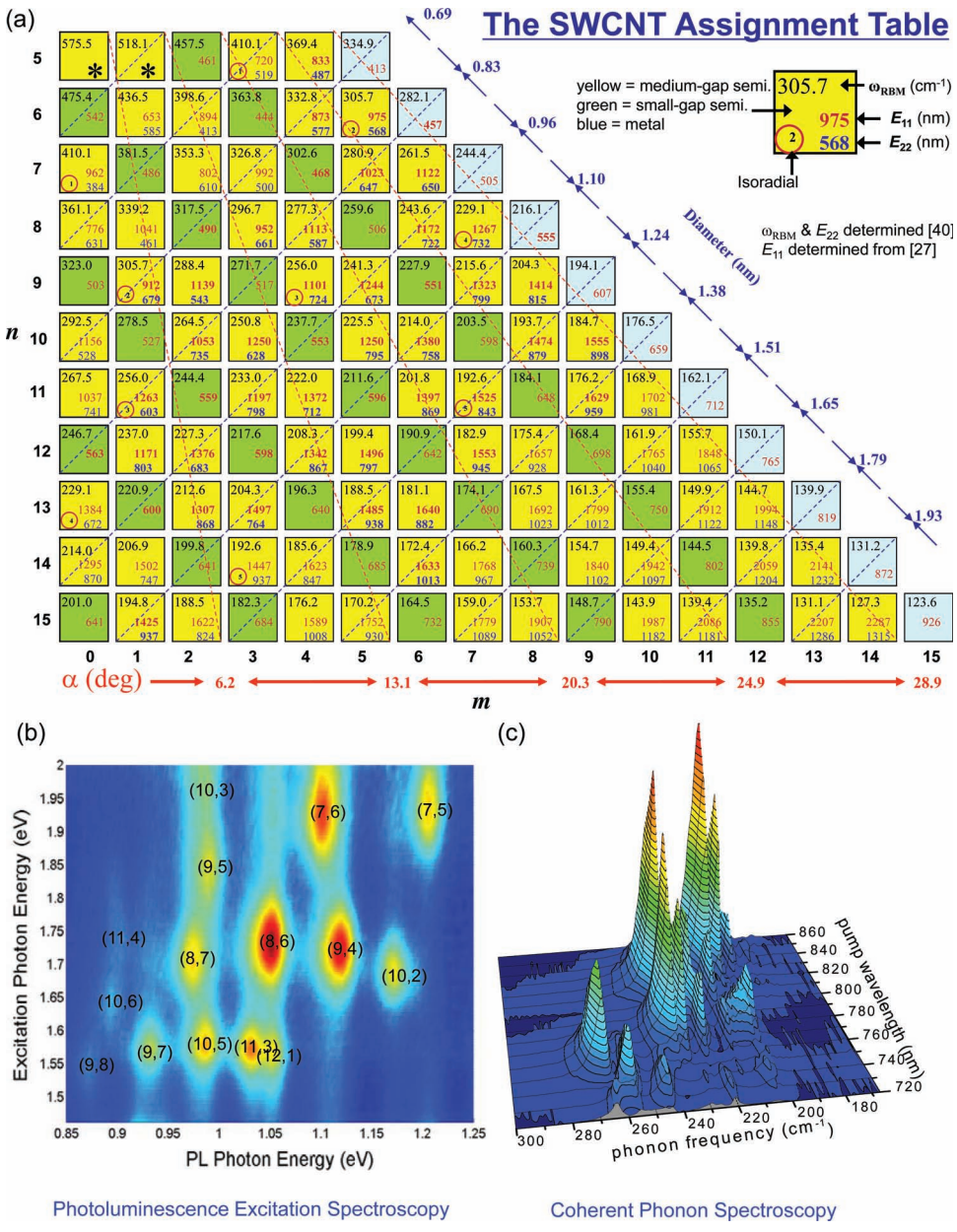

Figure 2. a) Sivarajan Chart for the electronic assignment of single-wall carbon nanotubes. Most experimental data is for SWCNT suspended in SDS. Each colored square represents a particular (n,m) species identified by n (left axis) and m (bottom axis). The color (yellow, green, and blue) of each square indicates its respective electronic type (medium-gap semiconductor, small-gap semiconductor, and metal). For each (n,m) species, the radial breathing mode (RBM) frequency (in cm–1) and the E11 resonance wavelength (in nm) are indicated. For semiconducting [(n – m) mod 3 = ±1] nanotubes, the E22 resonance wavelength (in nm) is also shown. The red circle in the bottom left corner of some entries represents isoradial (n,m) pairs of identical diameters; the pairs are matched with the number "i" inside the red circle. Values for RBM frequency and E22 are taken from ref. [40] Values for E11 are taken from ref. [27] Reproduced with permission from ref. [188]. Copyright 2004, Ramesh Sivarajan. b) Typical PLE map for HiPco nanotubes suspended in aqueous SDS. c) Resonant coherent phonon spectroscopy map (see Section 3 for more details).

ultracentrifugation (DGU), first employed for SWCNT separation by Arnold and co-workers in 2005.[193,194] This technique has since been used by many groups to effectively produce samples of only metallic nanotubes and semiconducting nanotubes, respectively.[56,195–198] The intrinsic differences in mass density of different-chirality nanotubes are primarily due to the varying diameter of the surfactant micelle and the binding affinities of different types of nanotubes for the surfactant. The separation is accomplished by subjecting surfactant-suspended SWCNTs in an aqueous suspension to travel through a mass density gradient via ultracentrifugation (≈200 000*g* for 18 hours). Due to the variation in density of the gradient, different density nanotubes will migrate towards different regions of the gradient, under the applied force of the centrifuge versus the buoyant density of the nanotube, until an equilibrium is reached. At this point, the nanotubes are now sufficiently separated in vertical

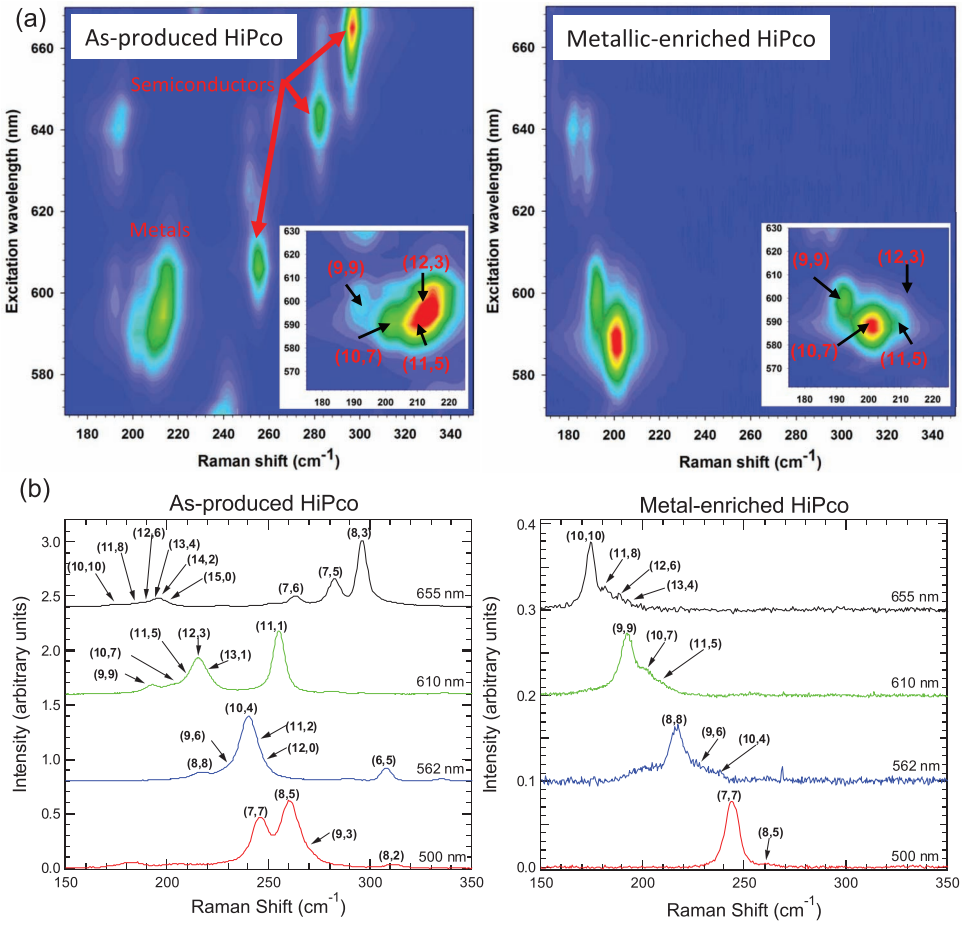

Figure 3. Raman spectroscopic evidence, comparing before (left) and after (right) the density-gradient ultracentrifugation process, for the enrichment of: a) "metallic" ($v = 0$) nanotubes, and in particular, b) armchair, or (n,n), carbon nanotubes. Adapted from Ref.[56]

distance in the gradient so that they may be extracted using simple fractionation techniques.

Hároz et al. have used DGU to prepare aqueous suspensions of nearly all metallic SWCNTs,[56] as evidenced through a variety of spectroscopy experiments, including PLE spectroscopy, absorption spectroscopy, and RRS spectroscopy (see **Figure 3**a). In particular, they used RRS spectroscopy of the radial breathing mode (RBM) phonons to quantitatively determine the chirality distribution of these metal-enriched samples.[56] This allowed them to identify the chiralities of nanotubes that are present in an ensemble sample by tuning the excitation photon energy through the energies of the E_{22} semiconducting and E_{11} metallic interband transitions. There is clear evidence that the main species that are enriched are armchair SWCNTs. For example, let us take the $2n + m = 21$ family (i.e., (10,1), (9,3), (8,5), and (7,7), where the (7,7) tube is the only truly metallic tube among them). The RRS data shown in Figure 3b suggests that the relative abundance, reflected in the relative peak intensities, increases with increasing chiral angle, α (see Figure 2a). This is truly striking considering the fact that the Raman intensity actually tends to decrease with increasing α due to the decreasing electron-phonon coupling strength.[199–201]

Hároz et al. further studied the absorption properties of a series of armchair-enriched SWCNT samples with different diameter distributions, prepared using DGU, exhibiting distinct colors, as shown in **Figure 4**, right.[202] The starting materials were synthesized by CoMoCAT (average diameter, d_{avg} = 0.83 nm), HiPco (batch no. 189.2, d_{avg} = 0.96 nm), HiPco (batch no. 188.2, d_{avg} = 1.1 nm), HiPco (batch no. 107, d_{avg} = 1.1 nm), laser ablation (NASA, d_{avg} = 1.38 nm), and arc-discharge (d_{avg} = 1.5 nm). On the left of Figure 4 is a typical, as-produced SWCNT sample, which looks black because it contains a wide assortment of metallic and semiconducting SWCNTs with different diameters, absorbing everywhere in the visible optical range.

The size-dependent colors of suspended colloidal particles have fascinated researchers, engineers, and artists for centuries, and it is now well accepted that there are two distinctly different coloration mechanisms. While quantum confinement always plays a fundamental role, the coloration mechanism depends on whether the particles are metallic or semiconducting. For metallic nanoparticles, their colors are determined by the free-carrier plasma resonance whose frequency depends on the electron density as well as the particle size and shape.[203] For semiconducting nanoparticles, the key parameter is the size-dependent fundamental bandgap (i.e., the separation between the top of the valence band (highest occupied molecular orbital (HOMO)) and the bottom of the conduction band (lowest unoccupied molecular orbital (LUMO))), which sensitively changes

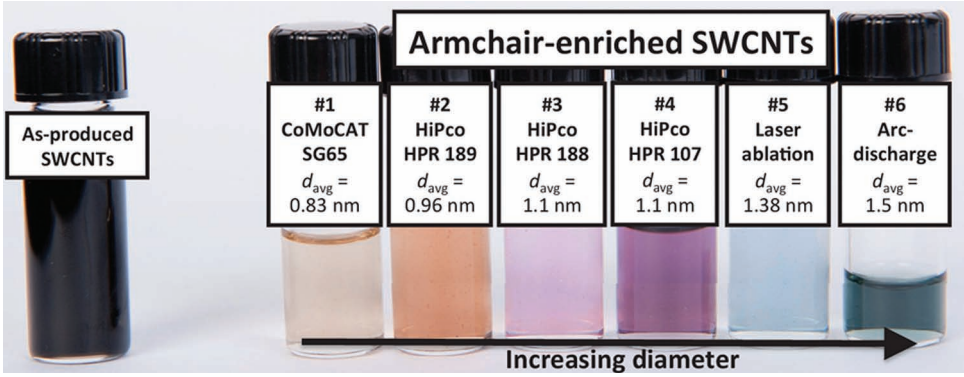

Figure 4. Pictures of armchair-enriched SWCNT suspensions. The black, "as-produced" vial on the left is typical of unsorted, SWCNT materials. On the right, various armchair-enriched samples with different diameters exhibit different, distinct colors. Adapted from Ref.[202]

with quantum confinement (i.e., size). Here, a novel case exists for armchair SWCNTs, suspended in aqueous medium, for which the origin of their color does not depend on the plasma resonance even though the individual particles are metallic.

The 1D Coulomb interaction differs significantly from systems with other dimensions. For example, the exciton binding energy becomes infinite in an ideal 1D electron-hole system.[204–206] In addition, the Sommerfeld factor, the ratio of the exciton continuum to the free electron-hole pair above the band edge, has been shown to be less than 1 in 1D systems.[207,208] 1D excitons in SWCNTs[209] seem to be even more peculiar. Early experimental PLE results (e.g., work by Weisman and Bachilo[27]) indicated that interband excitation energies are *higher* than those expected from band structure calculations based on simple tight-binding models. This blue shift is totally against our conventional wisdom that excitonic binding should red shift the excitation energy from the band edge. Ando's pioneering theoretical work[210,211] indicates that there is a significant blue shift from the single-particle bandgap (which is what tight-binding calculations yield) due to quasi-particle corrections. This blue shift is expected to exceed the excitonic binding energy, and thus, the net effect is a blue shift. A number of more recent theoretical studies[212–234] not only confirmed these predictions but also raised an array of new issues, questions, and predictions, including the intrinsic radiative lifetimes, the existence of "dark" excitons, and the stability of excitons in metallic carbon nanotubes. Two-photon PLE studies[235,236] have successfully determined the exciton binding energies to be very large (300–500 meV). Furthermore, recent temperature-dependent magneto-optical studies have provided new insight into the excitonic fine structure in SWCNTs,[117–121] including the direct measurement of dark-bright splitting values in individual SWCNTs.[106,107]

Although armchair SWCNTs are metallic in nature, the colors of their suspensions are not determined by their plasmonic properties as in metallic nanoparticles, nor by their bandgaps (which are zero) as in semiconducting nanoparticles. Rather, they are determined by a unique combination of band structure and selection rules for optical transitions.[202] For armchair SWCNTs, optical transitions between the linear bands are forbidden;[168,183] the minimum energy required for absorption is the separation between the first van Hove singularities, which is *not* the HOMO-LUMO separation. Near the resonant absorption energy, the optical transition is excitonic with a strongly suppressed continuum above the band edge, resulting in sharp absorption only in the vicinity of the excitonic optical transition.[229,237] This strong and narrow absorption peak for each armchair explains the apparent colors of armchair-enriched suspensions when viewed in the context of subtractive color theory.[202]

These metallically enriched SWCNT samples also provide an ideal system in which to study electron-phonon interactions and their consequences in Raman scattering spectra.[238–241] Of particular interest is the G-band, a Raman active optical phonon feature originating from the in-plane C–C stretching mode of sp^2-hybridized carbon. In SWCNTs, the G-band is split in two, the G^+ and G^- peaks, due to the curvature-induced inequality of the two bond-displacement directions. For $\nu = 0$ tubes, the higher-frequency mode (G^+) is a narrow Lorentzian peak, while the lower-frequency mode (G^-) is extremely broad. Earlier theoretical studies treated this broad G^- through a Breit–Wigner–Fano lineshape ascribed to the coupling of phonons with an electronic continuum[242] or low-frequency plasmons.[243] However, there is now accumulating consensus that the broad G^- peak is a softened and broadened longitudinal optical (LO) phonon feature, arising from Kohn anomalies.[49,51,238–241,244] Through either scenario, this broad G^- feature has conventionally been known as a "metallic" feature, indicating the presence of metallic tubes in the sample under study.

Hároz et al. have carried out detailed wavelength-dependent Raman measurements on a macroscopic ensemble of SWCNTs enriched in armchair nanotubes produced via DGU.[58] Their G-band spectra clearly showed that the broad G^- mode is absent for armchair nanotubes and only occurs for nonarmchair (i.e., $n \neq m$) "metallic" (or $\nu = 0$) nanotubes. Namely, the conventional method for identifying metallic nanotubes by observing a broad G^- peak does not apply to armchair nanotubes. This supports an earlier conclusion based on a small number of single-tube measurements,[55,244] as illustrated in **Figure 5** (Right), and negates some claims that armchair nanotubes also show a broad G^- feature.[245,246] Furthermore, this result firmly establishes a general correlation between G-band lineshape and nanotube structure due to the sampling of a statistically significant number ($\approx 10^{10}$) of nanotubes.

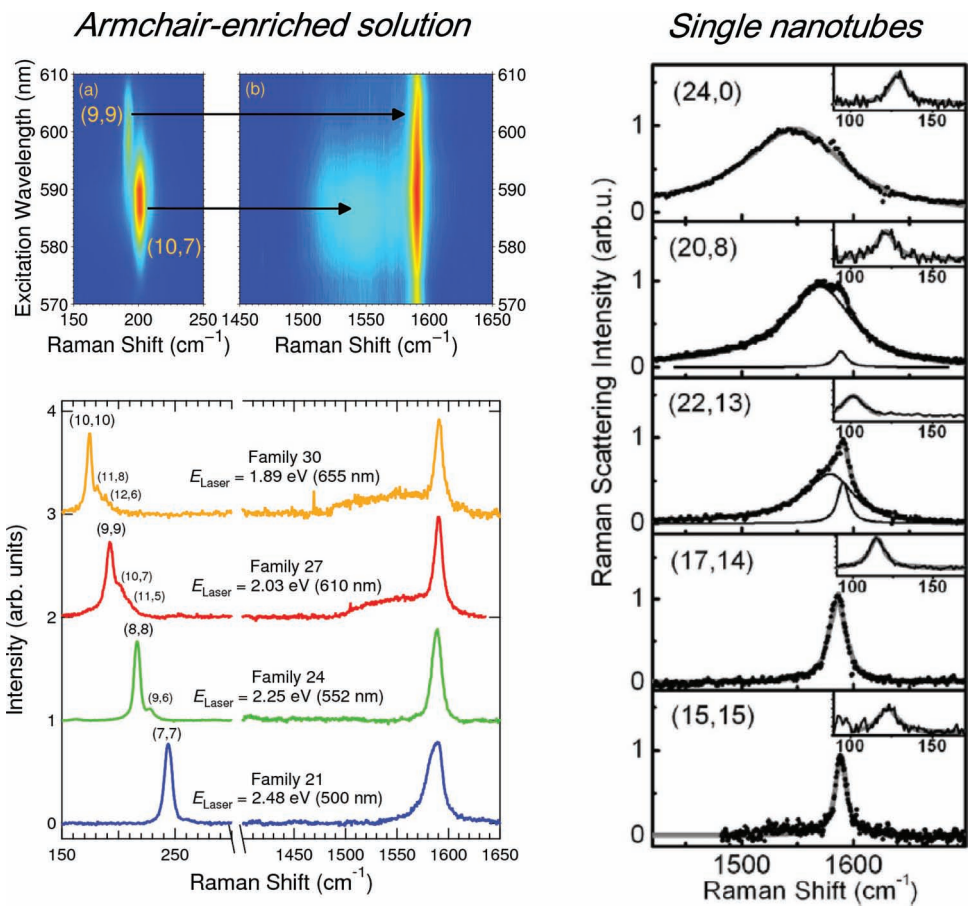

Figure 5. (Left,Top) Raman intensity for armchair-enriched SWCNTs as a function of Raman shift and excitation wavelength for Family $(2n + m) = 27$: a) radial breathing mode (RBM) region where two clear RBMs due to the (9,9) and (10,7) are observed; b) Corresponding G-band region where only the G^+ peak is observed when resonating primarily with the (9,9), and the appearance of the broad G^- coincides with the maximum of the (10,7) RBM. (Left,Bottom) Selected resonant Raman spectra at 655 nm, 610 nm, 552 nm, and 500 nm, where resonance primarily occurs with (10,10), (9,9), (8,8), and (7,7), respectively. In each case, the G-band reflects contribution mainly from the G^+ peak only. (Right) Resonant Raman spectrum for five individual "metallic" nanotubes ($\nu = 0$), the intrinsic response tends to show only the G^+ peak when the chiral angle approaches the armchair one. (Left) Adapted from Ref.[58] (Right) Reproduced with permission.[50] Copyright 2007, American Physical Society.

In Figure 5 (Top)(a), only two RBMs exist, arising from (9,9) and (10,7) nanotubes. The corresponding G-band [Figure 5 (Top)(b)] shows only a single G^+ peak centered at ≈1590 cm^{-1} at the longest excitation wavelengths (≈610 nm) corresponding to the resonance of the (9,9) RBM. As the wavelength is decreased, a broad G^- peak appears. This broad G^- peak, centered at ≈1550 cm^{-1}, reaches a maximum in intensity at ≈587 nm, which coincides with the RBM resonance maximum of the (10,7). The simultaneous appearance of the G^- peak with the Raman resonance maximum of the (10,7) and its absence with pure resonance with the (9,9) point out a clear correlation between (n,m) chirality and G-band lineshape. Namely, the broad G^- peak appears only in the presence of nonarmchair $\nu = 0$ nanotube species, and (n,n) armchair species show only one single, narrow peak. Figure 5 (Bottom) shows selected Raman spectra of the (7,7), (8,8), (9,9), and (10,10) armchair families taken at 500, 552, 610, and 655 nm excitations, respectively. These wavelengths are close to the general resonance maxima for each respective family. Data taken across a diameter range of 0.96–1.38 nm shown here clearly demonstrates that the appearance and dominance of a single G^+ feature is a general result and indicator for the predominance of armchair species in a SWCNT sample.

3. Ultrafast Bandgap Modulations in Carbon Nanotubes Via Coherent Lattice Vibrations

Because of the demand for higher-bandwidth communications, new schemes for high-speed optical modulations are being sought. Various switching schemes have been utilized to modify interband optical transitions in semiconductors at frequencies as high as 10^{12} s^{-1}, or THz.[247–251] Recently, Lim and co-workers[78,252] proposed and demonstrated a novel scheme for SWCNTs in which an optical beam is modulated by another optical beam (i.e., "all-optical" modulations) by the mediation of phonons. Since the phonons involved have high frequencies (several THz), and their phase and amplitude can be controlled in an arbitrary fashion by appropriately choosing the photon

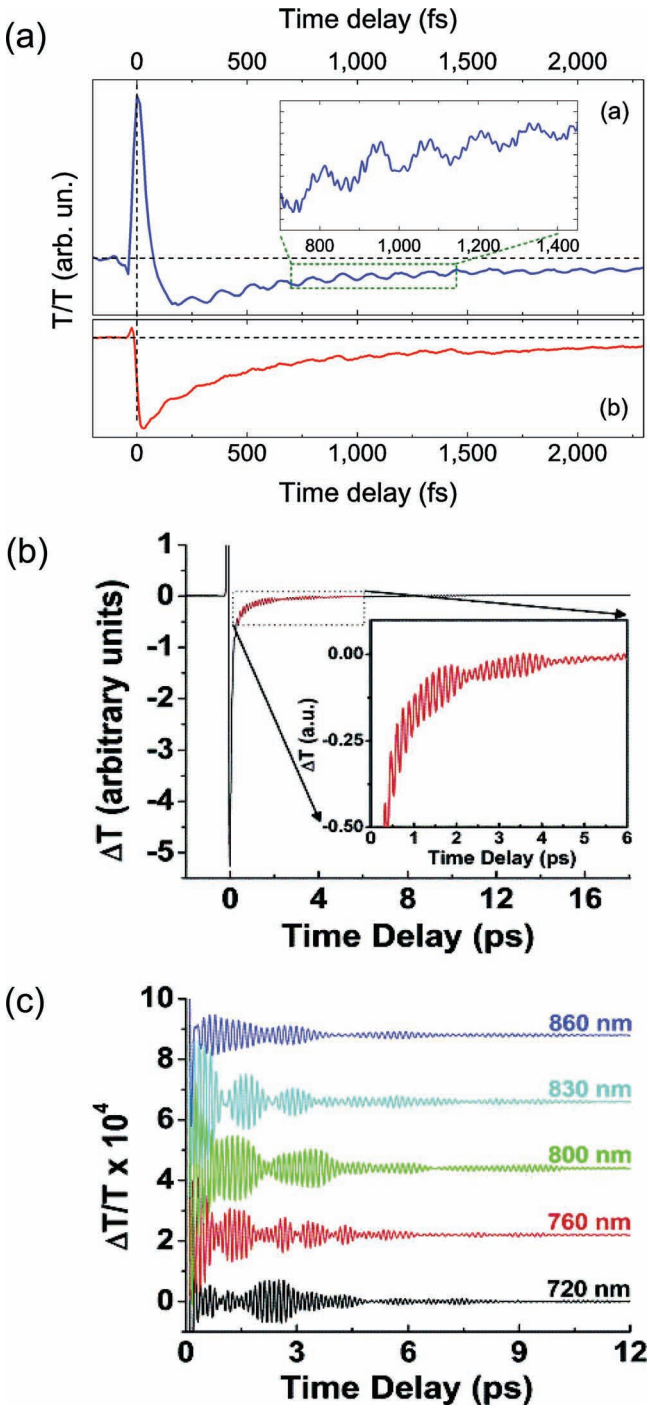

Figure 6. a) Raw pump-probe time-domain data taken with a 2.1 eV probe. The inset was taken using a higher sampling rate and shows that both the RBM and G modes can be resolved in the CP oscillations. b) Raw pump-probe time-domain data taken at an 800 nm center photon wavelength. The inset shows the region of the data taken between 0.3 and 6 ps, highlighting the CP contribution to the signal. c) CP oscillations excited and measured at five different photon energies. The individual traces are offset for clarity. (a) Reproduced with permission.[77] Copyright 2006, Macmillan Publishers Ltd: Nature Physics. (b,c) See Ref.[78] for more details.

energy of the pump pulse for a given (n,m) chirality,[253] this scheme naturally leads to ultrafast THz modulations.

Specifically, in ultrafast pump-probe experiments, several groups have succeeded in real-time observations of lattice vibrations, or coherent phonons (CPs), in SWCNTs.[72,77–78,82–84,86,89] Both the RBM and G-mode CPs have been clearly observed in the time domain (**Figure 6**a), as first evidenced by Gambetta et al.[77] In addition to revealing novel optical and electro-optical phenomena induced by the interplay of phonons and electrons, CP spectroscopy has many advantages over conventional continuous-wave (CW) characterization methods for SWCNTs, including: i) easy tuning of the center wavelength of the pump pulse, ii) simultaneous excitation of multiple vibrational modes due to the broad spectrum of the exciting pulse, iii) no Rayleigh scattering background at low frequency, iv) no photoluminescence signal, and v) direct measurement of vibrational dynamics including its phase information and dephasing times.

Figure 6b,c shows CP oscillations in SDS-suspended HiPco SWCNTs excited at different pump photon energies, reported by Lim et al.[78] The absolute amplitude of differential transmission oscillations is $\approx 10^{-4}$ near zero delay. Each trace in Figure 6b shows fast oscillations with a slowly varying envelope, or a beating pattern, indicating the coexistence of multiple, closely lying frequency components. The beating pattern sensitively changes with the wavelength of the pump, implying that the CP oscillations are dominated by RBMs that are resonantly excited via interband transitions, as is the case in RRS spectroscopy. To determine the frequencies of the excited phonons, a fast Fourier transform (FFT) of the time-domain oscillations was taken to produce CP spectra, shown in Figure 2c. Here, different (n,m) species show up as distinct peaks on this map, that is, a simultaneous function of excitation wavelength and RBM phonon frequency, similar to RRS maps[38] (see Figure 3a) or PLE maps (see Figure 2b). However, upon close examination, one finds noticeable differences between the CP data and CW RRS data. In particular, the CP spectra show a surprising double-peak dependence on the photon energy, which, as shown below, is a signature of RBM-CP-induced ultrafast bandgap modulations.

When the SWCNT lattice undergoes RBM oscillations, the diameter (d_t) periodically oscillates at frequency ω_{RBM}. This causes the bandgap, E_g, to also oscillate at ω_{RBM} (see **Figure 7**a) because E_g directly depends on the nanotube diameter (roughly $E_g \propto 1/d_t$). As a result, interband transition energies oscillate in time, leading to ultrafast modulations of optical constants at ω_{RBM}, which naturally leads to the oscillations in probe transmittance. Furthermore, these modulations imply that the absorption coefficient at fixed probe photon energy is modulated at ω_{RBM}. Correspondingly, the photon energy dependence of the CP signal for each RBM shows a *derivative-like* behavior, à la modulation spectroscopy[254] (see Figure 7b,c). This behavior can be modeled assuming that the CP signal intensity is proportional to the absolute value of the convoluted integral of the first derivative of a Lorentzian absorption line and a Gaussian probe beam profile. The results, shown as solid lines in Figure 7b,c, successfully reproduce the observed double peaks. The symmetric double-peak feature also confirms the excitonic nature of the absorption line (which will be modulated similarly to the bandgap due to an unaffected binding energy), in contrast to the asymmetric shape expected from the 1D van Hove singularity.[252]

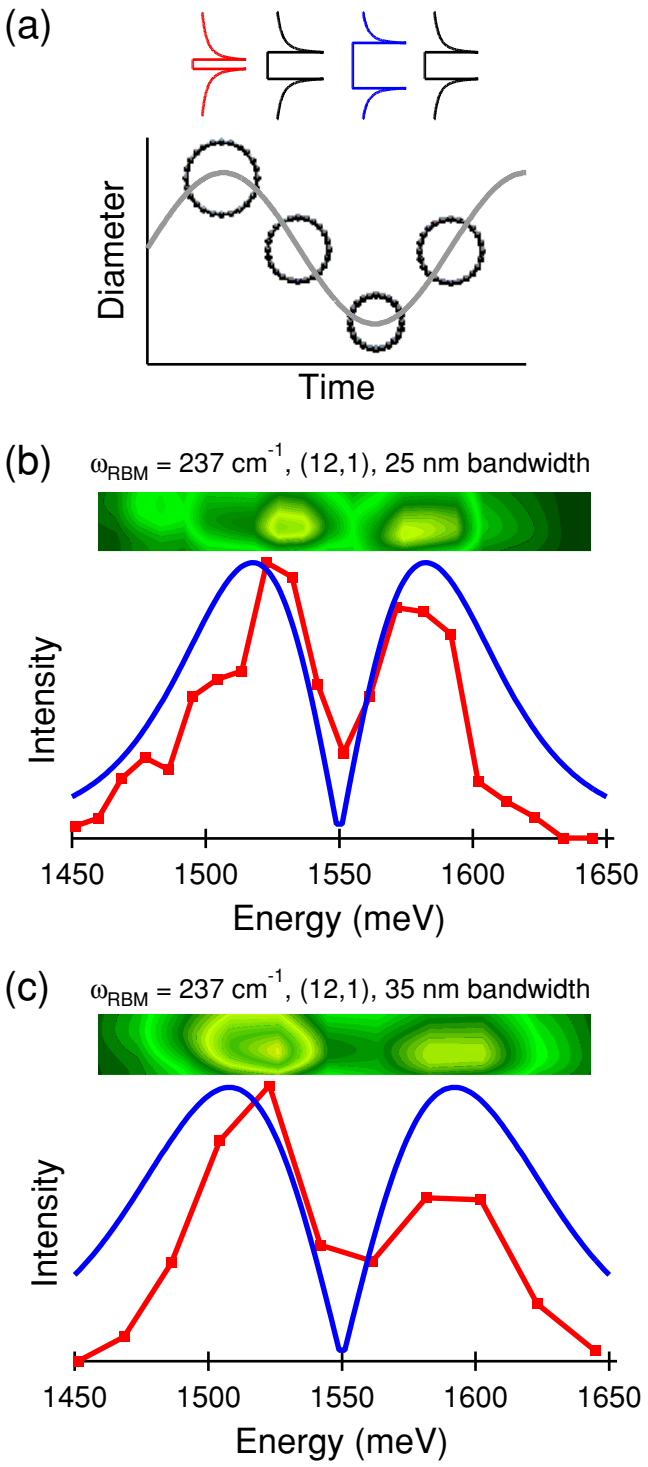

Figure 7. a) Diagram showing time-dependent bandgap due to the RBM of coherent lattice oscillations representing van Hove singularities oscillations. b,c) The photon energy dependence of the coherent phonon signal intensity (both contour and 2D plots) for the (12,1) tube with probe bandwidths of 25 nm (b) and 35 nm (c), together with theoretical curves (blue solid lines). See Ref.[78] for more details.

As mentioned in Section 2, recent advancements in post-growth separation techniques such as DGU allow researchers to study single-chirality samples. However, even when such techniques are not available, CPs of particular chirality SWCNTs can be selectively excited using the technique of pulse-shaping, as first demonstrated by Kim et al.[83] Using pre-designed trains of femtosecond optical pulses created through pulse-shaping, they selectively excited and probed RBM CPs of specific-chirality SWCNT within an ensemble sample of many different chiralities. Such CP data provided chirality-specific information on light absorption, phonon generation, and *phonon-induced band structure modulations*. In addition, by analyzing the probe wavelength dependence of the initial phase of the CPs for (11,3) SWCNTs, they proved that the nanotube diameter increases in response to ultrafast photoexcitation, which initiates coherent diameter oscillations.

The power of pulse-shaping is demonstrated in **Figure 8**. The left panel of Figure 8a shows typical CPs without pulse shaping. As before, the time-domain beating profiles reflect the simultaneous generation of several RBM frequencies, which are seen in the Fourier transform of the time-domain data in the right panel of Figure 8a. By introducing pulse-shaping, multiple pulses with different repetition rates are used to excite RBM oscillations, and, as shown in Figure 8b–e, chirality selectivity is successfully obtained. With the appropriate repetition rate of the pulse trains, a single, specific-chirality dominantly contributes to the signal, while other nanotubes are suppressed. For example, by choosing a pump repetition rate of 7.07 THz, only the (11,3) nanotubes can be excited, as seen in Figure 8b. Similarly, with a pump repetition rate of 6.69 THz, the (10,5) nanotubes are selectively excited, as seen in Figure 8c.

In this section, we have described an ultrafast optical process in which one optical beam initiates coherent bandgap oscillations in SWCNTs via coherent phonons, which in turn modulate the transmission of another optical beam, a promising scheme for ultrafast modulations and switching of optical beams. In addition, CP spectroscopy provides a useful tool for fundamental studies of phonon dynamics and electron-phonon interactions in SWCNTs with an ultrashort time scale. For example, the excitonic nature of interband optical excitation manifests itself in the detection process for the CP oscillations by the coupling with the broad spectrum of probe pulses. Furthermore, the expansion of the spectrum of femtosecond pulses into deep mid-infrared and visible ranges will allow one to explore large-diameter carbon nanotubes and metallic carbon nanotubes. Finally, the ability of CP measurements to trace the first derivative of the excitonic absorption peaks of specific chirality (n,m) will allow in-depth study of the lineshape of these resonances.

4. Optoelectronic Studies of Aligned Carbon Nanotube Films

As we illustrated in the previous sections, the 1D confinement of electrons and phonons in SWCNTs make them an ideal material for fundamental studies as well as potential applications. For a long time, however, successful experiments were limited to individual nanotubes. Recently, different methods have been developed for achieving a high-degree of alignment

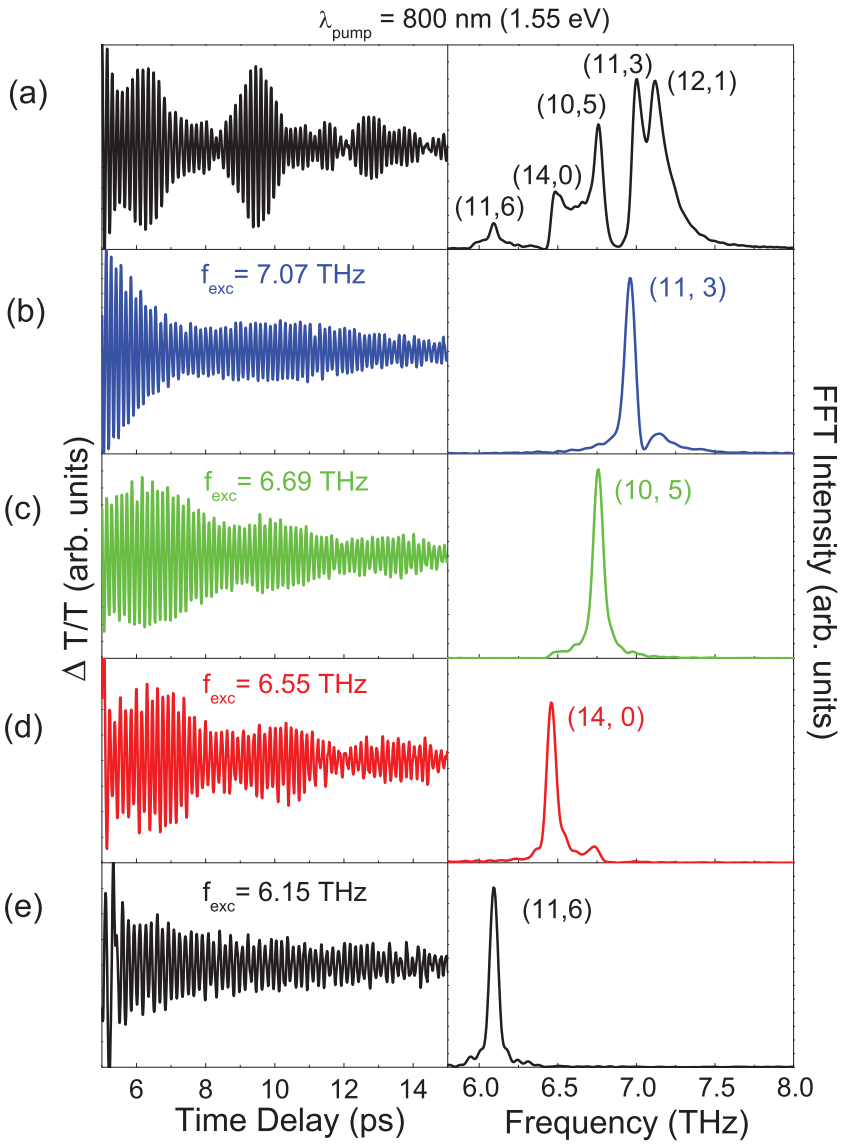

Figure 8. a) Left: Time-domain transmission modulations due to coherent RBM vibrations in ensemble SWCNTs solution generated using standard pump-probe techniques without pulse-shaping; Right: Fourier transformation of time-domain oscillations with chirality assigned peaks. b–f) Left: Time-domain coherent RBM oscillations selectively excited by multiple pulse trains via pulse shaping with corresponding repetition rates of 7.07–6.15 THz; Right: Fourier transformations of corresponding oscillations, with their dominant nanotube chirality (*n*,*m*) indicated. Reproduced with permission.[83] Copyright 2009, American Physical Society.

of SWCNTs on macroscopic scales, ideal for various device applications taking advantage of their 1D properties. These methods include, for example, "soft lithography" techniques[255] and "carpet" growth of vertically aligned SWCNTs by chemical vapor deposition (CVD),[256–259] which have already been used for different applications such as large-scale electronic devices;[260–262] see review by Lan et al.[263], for example. However, systematic studies on their anisotropic optical properties are still lacking, except for some polarization-dependent absorption studies on vertically aligned SWCNTs,[264] stretch-aligned SWCNTs,[265] and SWCNTs in solution that are aligned in high magnetic fields.[121,123]

In this section, we review recent studies of the AC (or optical or dynamic) conductivity in the terahertz (THz) frequency range (Section 4.1) and photovoltaic properties (Section 4.2) of large-area, highly aligned, CVD-grown films. These films have been obtained by vertical growth from 1 to 2 µm wide pads of catalyst (0.5 nm of Fe and 10 nm of Al_2O_3) defined by optical lithography and deposited using electron-beam evaporation, as illustrated in **Figure 9**a. SWCNTs were then grown in a hot-filament furnace by water assisted CVD,[256–259] as detailed in previous publications.[266–270] The length of the nanotubes was controlled by the exposure time and their average diameter was around 2.5 to 3 nm. The highly aligned nanotubes were then transferred onto sapphire substrates (see Figure 9b), producing homogeneous, cm^2-large films (Figure 9c) of highly *horizontally* aligned SWCNTs, with thicknesses of ≈2 µm. For photoconductivity experiments, ≈300 µm long and <1 µm thick individual lines were transferred on SiO_2 substrates using tweezers. Shadow masking techniques were then used to evaporate metallic electrodes (Au, Ti, and Pd) with a typical thickness of 50 nm and a channel length of 50 µm. These films present a very high degree of alignment on the microscopic scale as can be seen on scanning electron microscope images (Figure 9d) and very strong homogeneity at the macroscopic scale (Figure 9e).

4.1. Anisotropic Terahertz Transmission: Toward SWCNTs Polarizers

Much information on fundamental interactions in condensed matter, such as quantum confinement, disorder or electron-electron interactions, can be obtained from measurements of the AC conductivity $\sigma(\omega)$. A number of detailed theoretical calculations have underlined the effect of 1D confinement, in general or specifically in carbon nanotubes, taking into account disorder and interactions.[271–276] For example, metallic SWCNTs are expected to show a non Drude like behavior due to quantum fluctuations in 1D as well as an ω/T scaling of the conductivity in the Tomonaga–Luttinger liquid regime. As far as experimental studies are concerned, far-infrared and THz studies have produced contradicting results and interpretations. The most notable effect is the appearance of a broad absorption peak[277] around 4 THz (i.e., 135 cm^{-1} or 17 meV), assigned to a plasmon oscillation along the nanotube axis[278,279] or to the curvature-induced bandgaps in nonarmchair "metallic" SWCNTs,[277,280–282] without leading to any consensus.[283]

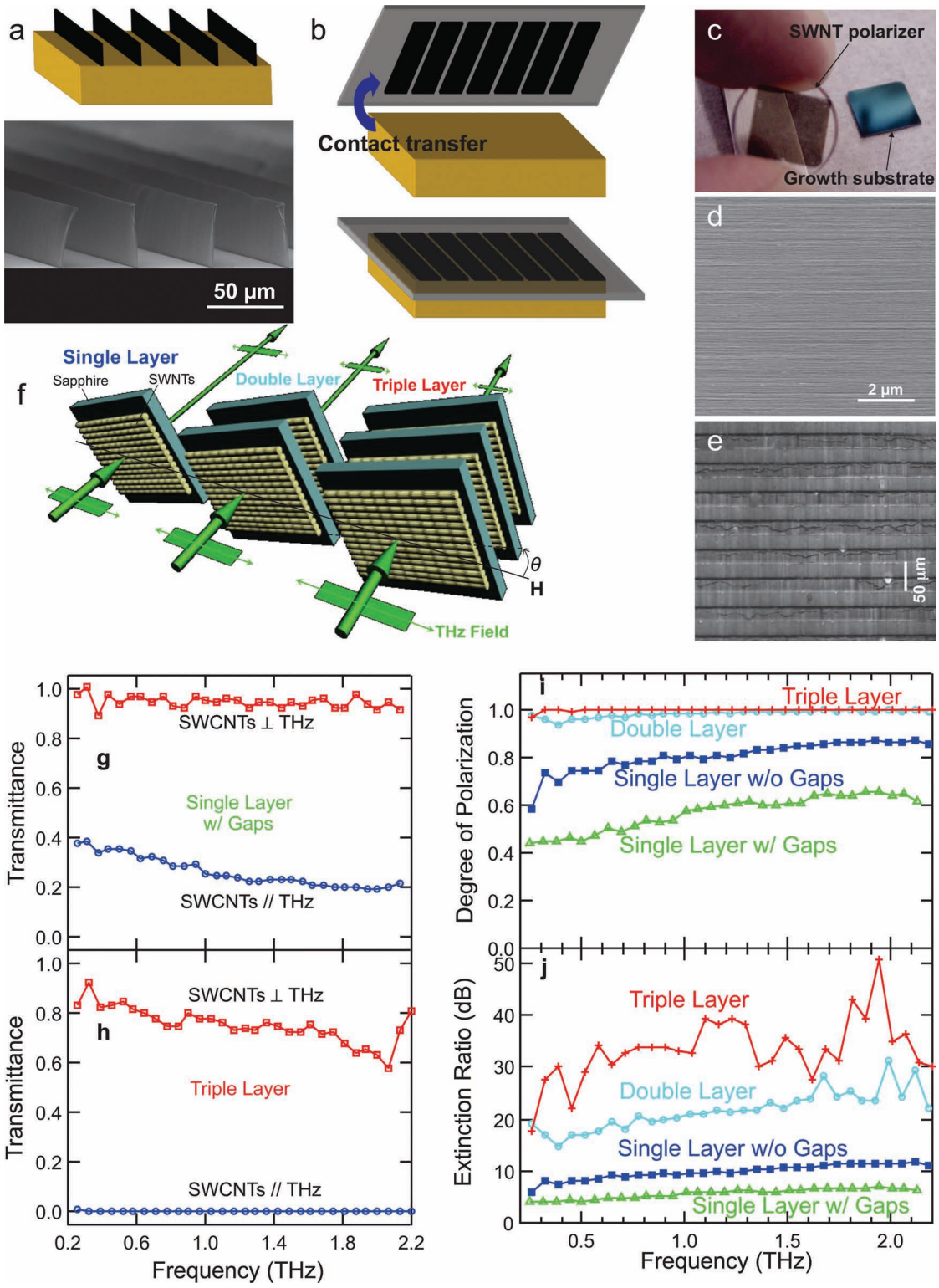

Figure 9. a) Schematic and SEM image of vertically grown SWCNT lines. b) Schematic of dry contact transfer of horizontally aligned SWCNTs onto the host substrate. c) Picture showing the 1 cm^2 film on a transparent sapphire substrate and original growth substrate. d) SEM image at high magnification showing the excellent alignment after transfer. (e) Optical image of the sample with gaps showing the film homogeneity. (f) Diagram of the measurement geometry showing the relative angle of the SWCNTs with respect to the THz polarization and the use of stacked films to increase the extinction ratio. THz transmittance spectra (0.2–2.2 THz range) for two extreme cases: g) one-layer SWCNT film with gaps corresponding to picture (e); h) three stacked layers without gaps; the red squares correspond to the SWCNT axis perpendicular the THz polarization and the blue dots to the parallel case. i,j) Degree of polarization (i), and extinction ratio (j) of the polarizers with different numbers of layers. Adapted from ref.[270] Copyright 2012, American Chemical Society.

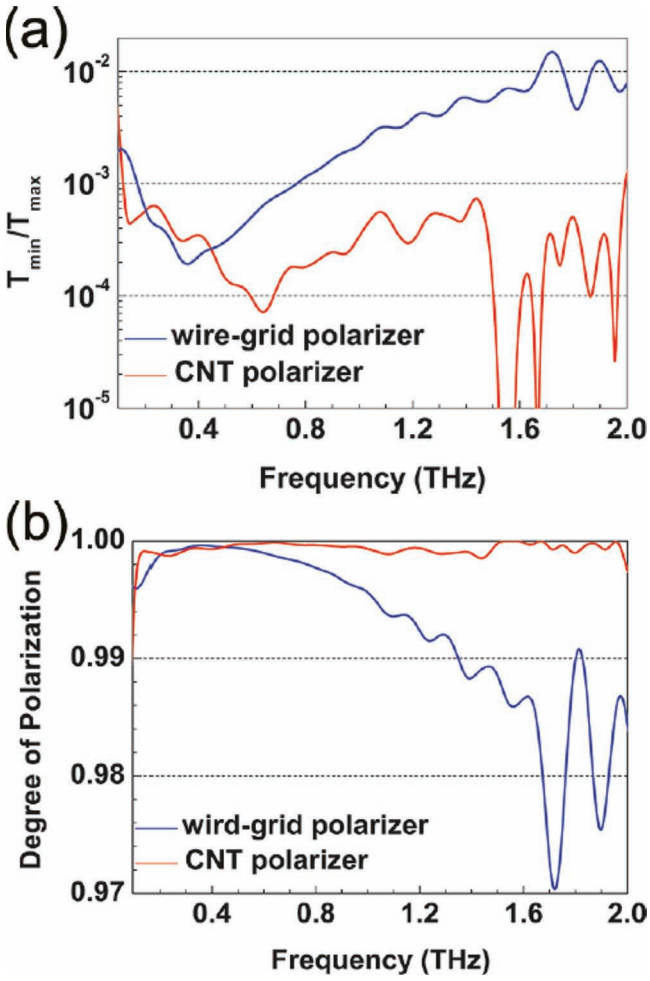

Figure 10. Comparison between the performances of a commercial free-standing wire-grid polarizer and a free-standing MWCNT sheet polarizer with optimized number of layers. a) The extinction ratios (T_{min}/T_{max}), and b) the degree of polarization are both better for the CNT polarizer in the 0.6–2 THz range. Reproduced with permission.[286] Copyright 2011, American Chemical Society.

Some of the previous studies have been performed on partially aligned samples, demonstrating some anisotropy in the optical conductivity in the THz range.[278,284,285] More recently, extreme anisotropy in the transmission has been reported for macroscopically aligned SWCNTs by Ren and co-workers[269,270] (Figure 9) as well as for macroscopically aligned MWCNT films by Kyoung et al. (**Figure 10**).[286] Strikingly, both studies reported performances comparable to commercial, wire-grid polarizers and presented two main advantages: i) a much stronger mechanical robustness, and ii) a broader-band THz absorption. This second point makes CNTs particularly attractive since the polarization properties are driven by the inherent 1D character of the film. Indeed, both SWCNT and MWCNT films exhibit a degree of polarization (DOP) of 99.9% and an extinction ratio (ER) as high as 35 dB. It should be also noted that, in addition to these advantages, sample fabrication does not rely on complex top-down approaches such as electron-beam lithography and chemical etching that are used to produce wire-grid polarizers.

Below, we will detail the work by Ren et al. on highly aligned SWCNT films on sapphire using a terahertz time-domain spectroscopy (THz-TDS) system.[269,270] The experimental setup used a Ti:sapphire femtosecond laser to excite a ZnTe crystal to generate coherent THz radiation, which was detected using a photoconductive antenna. The generated beam was further polarized by a wire-grid polarizer before being focused onto the sample. The sample was then rotated by an angle θ between the CNT axis and the polarization of the incident beam, as illustrated in Figure 9f. The CNT film transmission at different values of θ was then deduced by subtracting the absorption from reference measurements performed on sapphire substrates obtained from the same wafers. Up to three layers were stacked in order to optimize the absorption at $\theta = 0$ (i.e., SWCNTs parallel to the polarization axis) and achieve a maximum ER (Figure 9f).

It should be emphasized that no attenuation is observed when the SWCNTs are perpendicular to the polarization. The nematic order parameter was ≈1, as detailed by Ren et al.[269], implying the intrinsic nature of the polarization dependence. Figure 9g,h show the transmittance spectra between 0.2 and 2.2 THz after Fourier transforming the time-domain data. For a film with gaps between lines (i.e., line spacing is larger than the nanotube lengths, see Figure 9e), the transmission is already very small ($T = 0.2$–0.4) for the parallel configuration, whereas there is nearly complete transmission, $T \approx 1$ in the perpendicular case (Figure 9g). The decrease in transmission toward high frequencies is consistent with the finite-frequency absorption peak mentioned above. By stacking three layers fully covered with SWCNTs, the transmission drops down to 0 in the whole frequency range for the parallel configuration and remains very close to 1 in the perpendicular one (Figure 9h).

In order to further investigate the quality of these devices as polarizers,[287] the *DOP* and *ER*, respectively defined as $DOP = (T_{\perp} - T_{||})/(T_{\perp} - T_{||})$ and $ER = T_{||}/T_{\perp}$ were calculated (see Figure 9i,j). Due to the enhanced absorption when stacking layers and the intrinsic nature of the polarization dependence, both the *DOP* and *ER* are strongly increasing in the whole frequency range reaching values of $DOP = 99.9\%$ and $ER \simeq 33.4$ dB in the 0.4–2.2 THz range. Such a range is already much broader than typical commercial far-infrared polarizers, as illustrated in Figure 10,[286] and could be extended up to the mid-infrared[89] and visible[268] to design ultrawide spectral absorbers.

4.2. Photocurrent Generation at the Film/Electrode Interface

One of the promising optoelectronic applications of SWCNTs is solar technology/photodetection. Much of the interest is driven by the fact that SWCNTs can absorb light in virtually the entire visible spectral range (see Sections 1 and 2), due to their diameter-dependent optical transitions between sub-bands. In addition, intraband absorption in the infrared and THz in metallic and doped semiconducting nanotubes (see Section 4.1) is promising for ultrabroadband detection. The photodetection properties of SWCNTs have been studied for single tubes,[91,98,100,102,109,125,131,137] ensembles,[126–129,132–136,139–141,143,144,146,148,150–154]

and hybrid and composite structures.[130,138,142,145,147,149] Clear photovoltaic signals have been identified in clean SWCNT Schottky diodes,[91,131,137] *p-n* junctions,[100,102,109] and even metallic nanotubes[98] at the single-tube level. However, for macroscopic SWCNT films (either from single-wall or multiwall), various mechanisms have been proposed, including photodesorption,[127–128] bolometric effects,[132,140,150] and photothermoelectric effects.[148,151–153] The latter two effects have been observed in suspended films, whereas the photocurrents generated at the electrode-CNT film junctions have been assigned to photovoltaic effects at Schottky barrier junctions,[136,141,143–146] similar to single-tube experiments, despite the presence of metallic nanotubes and complete randomness of CNT orientations; one noticeable exception is the study by St-Antoine et al.,[153] who interpreted their results in terms of photothermoelectric effects between the CNT film and metal electrodes.

Here, we describe our recent study of broadband photodetection using the highly aligned, ultralong SWCNT films presented in the introduction of this section.[288] Because the nanotubes were ultralong (>300 μm), it was possible to use shadow masking, which avoided accidental doping, alignment deterioration, and further densification, which would have been introduced in standard photolithography processes. The samples were contacted with the current either parallel (with the same SWCNTs spanning both electrodes) or perpendicular to the nanotube orientation (with the current entirely relying on tube-tube junctions). We first performed scanning photocurrent microscopy (SPCM), illustrated in **Figure 11**a, using 660 nm and 1350 nm laser diodes as light sources. The laser beam was highly focused (≈1 μm spot diameter) on the sample with a typical power of 2 mW. The sample was kept in vacuum and scanned with two motorized stages along the focal plane axis. Sample positioning and laser focusing were achieved using a white-light source and a CCD camera, which were turned off during measurements. We then recorded $I(V)$ curves at each position, as well as the position-dependent open-circuit photovoltage (V_{OC}) or the short-circuit photocurrent (I_{SC}) (Figure 11b,c).

Figure 11 shows typical results for a device with two Au contacts with a current orientation parallel to the nanotube axis. Typical two-point $I(V)$ curves in the absence of light (not shown here) were linear and showed a resistance around 100 Ω (typical perpendicular resistance was a few kΩ measured for a different device). Under illumination, no change in resistance was observed but a strong photovoltage (or symmetrical photocurrent) was observed when the light was focused near the electrode edges, as shown in Figure 11b. While a positive photovoltage ($V_{OC} > 0$) develops near the left electrode, a negative V_{OC} arises near the right electrode. The photovoltage starts developing as far as ≈30 μm under the electrode. Note that this behavior is entirely reproducible along the width of the sample.

As expected from the very high degree of alignment of the film, the photosignal shows strong polarization dependence (Figure 11c), with a signal intensity ratio of ≈1/2, indicating the role of interband absorption in the measured signal. Moreover, the decay length of the signal when moving away from the electrode goes down to less than 10 μm when the photocurrent is collected perpendicular to the nanotube orientation on the same SWCNT film (Figure 11d). The amplitude is almost the same for both orientations (not shown here). We attribute this photoinduced signal to a photo-thermolectric (PTE) effect, which relies on the metal-induced doping gradient present in the film. Because of the doping gradient, the Seebeck coefficient in the channel is different from that under the electrode. When the light beam locally heats the film, a temperature gradient arises, which leads to the generation of a voltage. Self-consistent calculations reproduce this behavior well.[288] This one is noticeably different from previously reported PTE effects in carbon nanotube films; in particular as can be seen in Figure 11f, random networks need to be suspended and annealed in order to produce a Seebeck gradient intrinsic to the CNT film together with a heating by the laser giving rise to a local photovoltage;[148] whereas the photoresponse is assigned to a difference in thermopower between the film and the electrode when the device is in direct contact with the substrate.[152]

5. Summary and Outlook

We have reviewed some of the fascinating optical properties of single-wall carbon nanotubes that are promising for a variety of optoelectronic applications. During the last decade, various CW and ultrafast optical, magneto-optical, and terahertz spectroscopy studies have revealed unusual properties of one-dimensional carriers, excitons, and phonons in semiconducting and metallic nanotubes. Progress in post-growth separation methods has made significant impact on studies of (n,m)-dependent properties. Recent studies have shown that armchair, or $n = m$, nanotubes behave in a similar way to semiconducting nanotubes in terms of optical absorption, even though they electrical properties are drastically different. It has been shown, experimentally and theoretically, that coherent lattice vibrations in the radial breathing mode induce bandgap oscillations in carbon nanotubes at THz frequencies, opening up possibilities for novel ultrafast optical modulation schemes. Finally, aligned nanotubes have a wide range of optoelectronic applications, and we have reviewed only two aspects, terahertz devices and photodetectors, in this article.

Semiconducting single-wall carbon nanotubes are attracting particularly strong attention for developing light-emitting and detecting devices, because they are direct-bandgap systems. In addition, their diameter-dependent bandgaps can be utilized for unique multiwavelength devices. However, there are many challenges facing researchers in this area because macroscopic samples of aligned nanotubes of single chirality are still not available. Furthermore, they have shown rather strong Auger recombination, which prevents the creation of large density of electron-hole pairs, or population inversion, a prerequisite for lasing. Research on the optical spectroscopy of carbon nanotubes has produced a vast literature over the past 10 years, but most of these studies have been carried out under weak excitation in the quasi-equilibrium regime. In order to realize device-operating conditions, it is important to investigate their optical properties under highly non-equilibrium conditions. Many new studies have been appearing in recent years, including studies on graphene, to probe and assess their performance characteristics as optoelectronic materials under device-operating conditions by strongly driving them far from equilibrium, either electrically or optically, and examine their optical

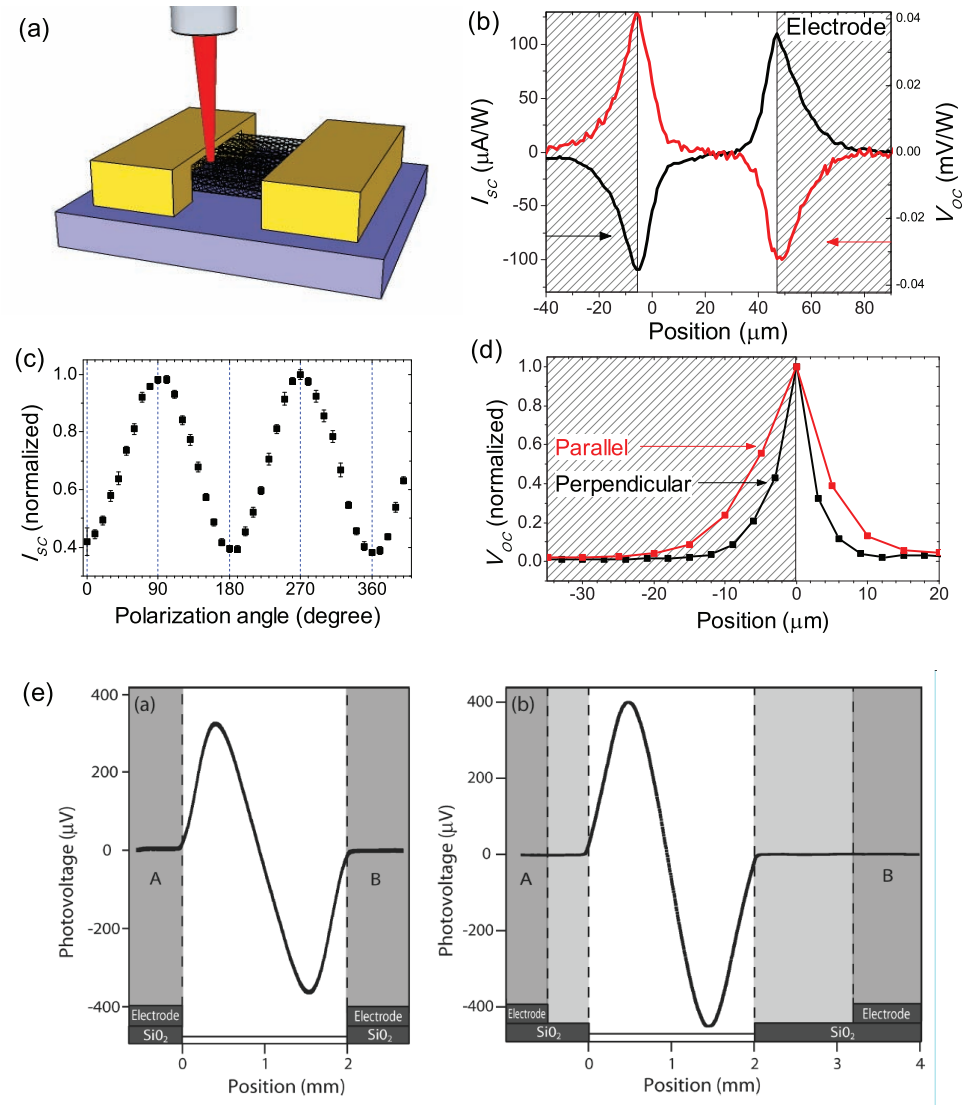

Figure 11. a) Schematic diagram of the scanning photocurrent measurement of highly aligned carbon nanotubes. b) Typical photoresponse at 1350 nm of a film with Au contacts showing strong maxima at the electrode edges for both the short-circuit photocurrent I_{sc} (right axis, red line) and the open-circuit photovoltage V_{oc} (left axis, blue line). c) Polarization dependence at 1350 nm of the photogenerated signal reaching a maximum when the polarization is parallel to the SWCNT axis. d) Comparison of the spatial dependence of the photocurrent showing that the signal starts appearing further from the electrode in parallel due to higher thermal conductivity; data are averaged along the width of the sample. e) Results obtained from a suspended, thin, random network of carbon nanotubes. The photo-thermoelectric voltage develops in the suspended part due to a strong thermal coupling to the substrate, which acts as a heat sink, and a doping gradient induced by preliminary current annealing. (e) Reproduced with permission.[148] Copyright 2009 American Chemical Society.

properties in highly non-equilibrium situations. These results will form the knowledge base needed for preparing the next generation of solid-state devices as well as for understanding out-of-equilibrium properties of interacting, confined carriers at low dimensions.

Acknowledgements

This work was supported by the National Science Foundation through Grant Nos. DMR-1006663, DMR-1105437, and OISE-0968405, the Department of Energy BES Program through Grant No. DEFG02-06ER46308, the Robert A. Welch Foundation through Grant No. C-1509, and Lockheed–Martin Corporation. We thank our collaborators who contributed to the work presented in this review article: L. G. Booshehri, Q. Zhang, L. Ren, J. Shaver, B. Y. Lu, W. D. Rice, T. Arikawa, J. G. Duque, S. K. Doorn, Y.-S. Lim, K.-J. Yee, G. D. Sanders, C. J. Stanton, R. Saito, C. L. Pint, A. A. Belyanin, I. Kawayama, M. Tonouchi, A. Cummings, and F. Léonard.

Received: May 1, 2012
Revised: June 28, 2012
Published online: August 22, 2012

[1] S. Iijima, T. Ichihashi, *Nature* **1993**, *363*, 603.
[2] D. S. Bethune, C. H. Klang, M. S. de Vries, G. Gorman, R. Savoy, J. Vazquez, R. Beyers, *Nature* **1993**, *363*, 605.
[3] C. L. Kane, E. J. Mele, *Phys. Rev. Lett.* **1997**, *78*, 1932.
[4] C. Kane, L. Balents, M. P. A. Fisher, *Phys. Rev. Lett.* **1997**, *79*, 5086.
[5] L. Balents, R. Egger, *Phys. Rev. Lett.* **2000**, *85*, 3464.
[6] L. Balents, *Phys. Rev. B: Condens. Matter* **2000**, *61*, 4429.
[7] A. De Martino, R. Egger, K. Hallberg, C. A. Balseiro, *Phys. Rev. Lett.* **2002**, *88*, 206402.
[8] L. S. Levitov, A. M. Tsvelik, *Phys. Rev. Lett.* **2003**, *90*, 016401.
[9] S. Bellucci, J. González, P. Onorato, *Phys. Rev. Lett.* **2005**, *95*, 186403.
[10] F. Guinea, *Phys. Rev. Lett.* **2005**, *94*, 116804.
[11] B. Dóra, M. Gulácsi, F. Simon, H. Kuzmany, *Phys. Rev. Lett.* **2007**, *99*, 166402.
[12] B. Dóra, M. Gulácsi, J. Koltai, V. Zólyomi, J. Kürti, F. Simon, *Phys. Rev. Lett.* **2008**, *101*,106408.
[13] V. V. Mkhitaryan, Y. Fang, J. M. Gerton, E. G. Mishchenko, M. E. Raikh, *Phys. Rev. Lett.* **2008**, *101*, 256401.
[14] E. G. Mishchekno, O. A. Starykh, *Phys. Rev. Lett.* **2011**, *107*, 116804.
[15] P. Avouris, Z. Chen, V. Perebeinos, *Nat. Nanotechnol.* **2007**, *2*, 605.
[16] P. Avouris, M. Freitag, V. Perebeinos, *Nat. Photonics* **2008**, *2*, 341.
[17] F. Léonard, *The Physics of Carbon Nanotube Devices*, William Andrew, Norwich NY, **2009**.
[18] R. Saito, G. Dresselhaus, M. S. Dresselhaus, *Physical Properties of Carbon Nanotubes*, Imperial College Press, London, **1998**.
[19] *Carbon Nanotubes: Synthesis, Structure, Properties, and Applications*, (Eds: M. S. Dresselhaus, G. Dresselhaus, P. Avouris), *Topics in Applied Physics No. 18*, Springer, Berlin,**2001**.
[20] S. Reich, C. Thomsen, J. Maultzsch, *Carbon Nanotubes: Basic Concepts and Physical Properties*, Wiley-VCH, Weinheim Germany **2004**.
[21] *Carbon Nanotubes: Properties and Applications*, (Ed: M. J. O'Connell), CRC Press, Taylor & Francis Group, Boca Raton, FL **2006**.
[22] *Carbon Nanotubes: Advanced Topics in the Synthesis, Structure, Properties and Applications*, (Eds: A. Jorio, G. Dresselhaus, M. S. Dresselhaus), Springer, Berlin, **2008**.
[23] M. J. O'Connell, S. M. Bachilo, C. B. Huffman, V. C. Moore, M. S. Strano, E. H. Hároz, K. L. Rialon, P. J. Boul, W. H. Noon, C. Kittrell, J. Ma, R. H. Hauge, R. B. Weisman, R. E. Smalley, *Science* **2002**, *297*, 593.
[24] S. M. Bachilo, M. S. Strano, C. Kittrell, R. H. Hauge, R. E. Smalley, R. B. Weisman, *Science* **2002**, *298*, 2361.
[25] S. Lebedkin, F. Hennrich, T. Skipa, M. M. Kappes, *J. Phys. Chem. B* **2003**, *107*, 1949.
[26] J. Lefebvre, Y. Homma, P. Finnie, *Phys. Rev. Lett.* **2003**, *90*, 217401.
[27] R. B. Weisman, S. M. Bachilo, *Nano Lett.* **2003**, *3*, 1235.
[28] Y. Miyauchi, S. Chiashi, Y. Murakami, Y. Hayashida, S. Maruyama, *Chem. Phys. Lett.* **2004**, *387*, 198.
[29] O. N. Torrens, D. E. Milkie, M. Zheng, J. M. Kikkawa, *Nano Lett.* **2006**, *6*, 2864.
[30] P. H. Tan, A. G. Rozhin, T. Hasan, P. Hu, V. Scardaci, W. I. Milne, A. C. Ferrari, *Phys. Rev. Lett.* **2007**, *99*, 137402.
[31] O. Kiowski, K. Arnold, S. Lebedkin, F. Hennrich, M. M. Kappes, *Phys. Rev. Lett.* **2007**, *99*, 237402.
[32] O. N. Torrens, M. Zheng, J. M. Kikkawa, *Phys. Rev. Lett.* **2008**, *101*, 157401.
[33] Y. Murakami, J. Kono, *Phys. Rev. Lett.* **2009**, *102*, 037401.
[34] Y. Murakami, J. Kono, *Phys. Rev. B: Condens. Matter* **2009**, *80*, 035432.
[35] J. A. Fagan, J. Y. Huh, J. R. Simpson, J. L. Blackburn, J. M. Holt, B. A. Larsen, A. R. H. Walker, *ACS Nano* **2011**, *5*, 3943.
[36] A. Jorio, A. G. Souza Filho, G. Dresselhaus, M. S. Dresselhaus, A. K. Swan, M. S. Ünlü, B. B. Goldberg, M. A. Pimenta, J. H. Hafner, C. M. Lieber, R. Saito, *Phys. Rev. B: Condens. Matter* **2002**, *65*, 155412.
[37] H. Telg, J. Maultzsch, S. Reich, F. Hennrich, C. Thomsen, *Phys. Rev. Lett.* **2004**, *93*, 177401.
[38] S. K. Doorn, D. A. Heller, P. W. Barone, M. L. Usrey, M. S. Strano, *Appl. Phys. A* **2004**, *78*, 1147.
[39] C. Fantini, A. Jorio, M. Souza, M. S. Strano, M. S. Dresselhaus, M. A. Pimenta, *Phys. Rev. Lett.* **2004**, *93*, 147406.
[40] J. Maultzsch, H. Telg, S. Reich, C. Thomsen, *Phys. Rev. B: Condens. Matter* **2005**, *72*, 205438.
[41] S. K. Doorn, M. J. O'Connell, L. Zheng, Y. T. Zhu, S. Huang, J. Liu, *Phys. Rev. Lett.* **2005**, *94*, 016802.
[42] J. Jiang, R. Saito, A. Grüneis, S. G. Chou, G. G. Samsonidze, A. Jorio, G. Dresselhaus, M. S. Dresselhaus, *Phys. Rev. B: Condens. Matter* **2005**, *71*, 205420.
[43] J. C. Meyer, M. Paillet, T. Michel, A. Moréac, A. Neumann, G. S. Duesberg, S. Roth, J.-L. Sauvajol, *Phys. Rev. Lett.* **2005**, *95*, 217401.
[44] A. Jorio, C. Fantini, M. A. Pimenta, R. B. Capaz, G. G. Samsonidze, G. Dresselhaus, M. S. Dresselhaus, J. Jiang, N. Kobayashi, A. Grüneis, R. Saito, *Phys. Rev. B: Condens. Matter* **2005**, *71*, 075401.
[45] M. Paillet, T. Michel, J. C. Meyer, V. N. Popov, L. Henrard, S. Roth, J.-L. Sauvajol, *Phys. Rev. Lett.* **2006**, *96*, 257401.
[46] H. Son, A. Reina, G. G. Samsonidze, R. Saito, A. Jorio, M. S. Dresselhaus, J. Kong, *Phys. Rev. B: Condens. Matter* **2006**, *74*, 073406.
[47] Y. Yin, A. N. Vamivakas, A. G. Walsh, S. B. Cronin, M. S. Ünlü, B. B. Goldberg, A. K. Swan, *Phys. Rev. Lett.* **2007**, *98*, 037404.
[48] F. Wang, W. Liu, Y. Wu, M. Y. Sfeir, L. Huang, J. Hone, S. O'Brien, L. E. Brus, T. F. Heinz, Y. R. Shen, *Phys. Rev. Lett.* **2007**, *98*, 047402.
[49] K. T. Nguyen, A. Gaur, M. Shim, *Phys. Rev. Lett.* **2007**, *98*, 145504.
[50] Y. Wu, J. Maultzsch, E. Knoesel, B. Chandra, M. Huang, M. Y. Sfeir, L. E. Brus, J. Hone, T. F. Heinz, *Phys. Rev. Lett.* **2007**, *99*, 027402.
[51] H. Farhat, H. Son, G. G. Samsonidze, S. Reich, M. S. Dresselhaus, J. Kong, *Phys. Rev. Lett.* **2007**, *99*, 145506.
[52] J. C. Tsang, M. Freitag, V. Perebeinos, J. Liu, P. Avouris, *Nat. Nanotechnol.* **2007**, *2*, 725.
[53] M. Oron-Carl, R. Krupke, *Phys. Rev. Lett.* **2008**, *100*, 127401.
[54] M. Fouquet, H. Telg, J. Maultzsch, Y. Wu, B. Chandra, J. Hone, T. F. Heinz, C. Thomsen, *Phys. Rev. Lett.* **2009**, *102*, 075501.
[55] T. Michel, M. Paillet, D. Nakabayashi, M. Picher, V. Jourdain, J. C. Meyer, A. A. Zahab, J.-L. Sauvajol, *Phys. Rev. B: Condens. Matter* **2009**, *80*, 245416.
[56] E. H. Hároz, W. D. Rice, B. Y. Lu, S. Ghosh, R. H. Hauge, R. B. Weisman, S. K. Doorn, J. Kono, *ACS Nano* **2010**, *4*, 1955.
[57] J. G. Duque, H. Chen, A. K. Swan, A. P. Shreve, S. Kilina, S. Tretiak, X. Tu, M. Zheng, S. K. Doorn, *ACS Nano* **2011**, *5*, 5233.
[58] E. H. Hároz, J. G. Duque, W. D. Rice, C. G. Densmore, J. Kono, S. K. Doorn, *Phys. Rev. B: Condens. Matter* **2011**, *84*, 121403(R).
[59] G. N. Ostojic, S. Zaric, J. Kono, M. S. Strano, V. C. Moore, R. H. Hauge, R. E. Smalley, *Phys. Rev. Lett.* **2004**, *92*, 117402.
[60] L. Huang, H. N. Pedrosa, T. D. Krauss, *Phys. Rev. Lett.* **2004**, *93*, 017403.
[61] J. Kono, G. N. Ostojic, S. Zaric, M. S. Strano, V. C. Moore, J. Shaver, R. H. Hauge, R. E. Smalley, *Appl. Phys. A* **2004**, *78*, 1093.
[62] A. Hagen, G. Moos, V. Talalaev, T. Hertel, *Appl. Phys. A* **2004**, *78*, 1137.
[63] Y.-Z. Ma, J. Stenger, J. Zimmerman, S. M. Bachilo, R. E. Smalley, R. B. Weisman, G. R. Fleming, *J. Chem. Phys.* **2004**, *120*, 3368.
[64] F. Wang, G. Dukovic, L. E. Brus, T. F. Heinz, *Phys. Rev. Lett.* **2004**, **92**, 177402.

[65] R. J. Ellingson, C. Engtrakul, M. Jones, M. Samec, G. Rumbles, A. J. Nozik, M. J. Heben, *Phys. Rev. B: Condens. Matter* **2005**, *71*, 115444.
[66] S. Reich, M. Dworzak, A. Hoffmann, C. Thomsen, M. S. Strano, *Phys. Rev. B: Condens. Matter* **2005**, *71*, 033402.
[67] F. Wang, G. Dukovic, E. Knoesel, L. E. Brus, T. F. Heinz, *Phys. Rev. B: Condens. Matter* **2004**, *70*, 241403(R).
[68] A. Maeda, S. Matsumoto, H. Kishida, T. Takenobu, Y. Iwasa, M. Shiraishi, M. Ata, H. Okamoto, *Phys. Rev. Lett.* **2005**, *94*, 047404.
[69] C.-X. Sheng, Z. V. Vardeny, B. Dalton, R. H. Baughman, *Phys. Rev. B: Condens. Matter* **2005**, *71*, 125427.
[70] S. G. Chou, F. Plentz, J. Jiang, R. Saito, D. Nezich, H. B. Ribeiro, A. Jorio, M. A. Pimenta, G. G. Samsonidze, A. P. Santos, M. Zheng, G. B. Onoa, E. D. Semke, G. Dresselhaus, M. S. Dresselhaus, *Phys. Rev. Lett.* **2005**, *94*, 127402.
[71] Y.-Z. Ma, L. Valkunas, S. L. Dexheimer, S. M. Bachilo, G. R. Fleming, *Phys. Rev. Lett.* **2005**, *94*, 157402.
[72] C. Manzoni, A. Gambetta, E. Menna, M. Meneghetti, G. Lanzani, G. Cerullo, *Phys. Rev. Lett.* **2005**, *94*, 207401.
[73] J. S. Lauret, C. Voisin, S. Berger, G. Cassabois, C. Delalande, P. Roussignol, L. Goux-Capes, A. Filoramo, *Phys. Rev. B: Condens. Matter* **2005**, *72*, 113413.
[74] A. Hagen, M. Steiner, M. B. Raschke, C. Lienau, T. Hertel, H. Qian, A. J. Meixner, A. Hartschuh, *Phys. Rev. Lett.* **2005**, *95*, 197401.
[75] S. G. Chou, M. F. DeCamp, J. Jiang, G. G. Samsonidze, E. B. Barros, F. Plentz, A. Jorio, M. Zheng, G. B. Onoa, E. D. Semke, A. Tokmakoff, R. Saito, G. Dresselhaus, M. S. Dresselhaus, *Phys. Rev. B: Condens. Matter* **2005**, *72*, 195415.
[76] G. N. Ostojic, S. Zaric, J. Kono, V. C. Moore, R. H. Hauge, R. E. Smalley, *Phys. Rev. Lett.* **2005**, *94*, 097401.
[77] A. Gambetta, C. Manzoni, E. Menna, M. Meneghetti, G. Cerullo, G. Lanzani, S. Tretiak, A. Piryatinski, A. Saxena, R. L. Martin, A. R. Bishop, *Nat. Phys.* **2006**, *2*, 515.
[78] Y.-S. Lim, K.-J. Yee, J.-H. Kim, J. Shaver, E. H. Hároz, J. Kono, S. K. Doorn, R. H. Hauge, R. E. Smalley, *Nano Lett.* **2006**, *6*, 2696.
[79] Y. Hashimoto, Y. Murakami, S. Maruyama, J. Kono, *Phys. Rev. B: Condens. Matter* **2007**, *75*, 245408.
[80] D. Song, F. Wang, G. Dukovic, M. Zheng, E. D. Semke, L. E. Brus, T. F. Heinz, *Phys. Rev. Lett.* **2008**, *100*, 225503.
[81] K. Kang, T. Ozel, D. G. Cahill, M. Shim, *Nano Lett.* **2008**, *8*, 4642.
[82] K. Kato, K. Ishioka, M. Kitajima, J. Tang, R. Saito, H. Petek, *Nano Lett.* **2008**, *8*, 3102.
[83] J.-H. Kim, K.-J. Han, N.-J. Kim, K.-J. Yee, Y.-S. Lim, G. D. Sanders, C. J. Stanton, L. G. Booshehri, E. H. Hároz, J. Kono, *Phys. Rev. Lett.* **2009**, *102*, 037402.
[84] L. Lüer, C. Gadermaier, J. Crochet, T. Hertel, D. Brida, G. Lanzani, *Phys. Rev. Lett.* **2009**, *102*, 127401.
[85] I. Chatzakis, H. Yan, D. Song, S. Berciaud, T. F. Heinz, *Phys. Rev. B: Condens. Matter* **2011**, *83*, 205411.
[86] J.-H. Kim, K.-J. Yee, Y.-S. Lim, L. G. Booshehri, E. H. Hároz, J. Kono, **2012**, arXiv:1106.2858v1.
[87] D. T. Nguyen, C. Voisin, P. Roussignol, C. Roquelet, J. S. Lauret, G. Cassabois, *Phys. Rev. Lett.* **2011**, *107*, 127401.
[88] S. M. Santos, B. Yuma, S. Berciaud, J. Shaver, M. Gallart, P. Gilliot, L. Cognet, B. Lounis, *Phys. Rev. Lett.* **2011**, *107*, 187401.
[89] L. G. Booshehri, C. L. Pint, G. D. Sanders, L. Ren, C. Sun, E. H. Hároz, J.-H. Kim, K.-J. Yee, Y.-S. Lim, R. H. Hauge, C. J. Stanton, J. Kono, *Phys. Rev. B: Condens. Matter* **2011**, *83*, 195411.
[90] J. J. Crochet, S. Hoseinkhani, L. Lüer, T. Hertel, S. K. Doorn, G. Lanzani, *Phys. Rev. Lett.* **2011**, *107*, 257402.
[91] M. Freitag, Y. Martin, J. A. Misewich, R. Martel, P. Avouris, *Nano Lett.* **2003**, *3*, 1067.
[92] A. Hartschuh, E. J. Sánchez, X. S. Xie, L. Novotny, *Phys. Rev. Lett.* **2003**, *90*, 095503.
[93] J. A. Misewich, R. Martel, P. Avouris, J. C. Tsang, S. Heinze, J. Tersoff, *Science* **2003**, *300*, 783.
[94] A. Hartschuh, H. N. Pedrosa, L. Novotny, T. D. Krauss, *Science* **2003**, *301*, 1354.
[95] J. Lefebvre, J. M. Fraser, P. Finnie, Y. Homma, *Phys. Rev. B: Condens. Matter* **2004**, *69*, 075403.
[96] H. Htoon, M. J. O'Connell, P. J. Cox, S. K. Doorn, V. I. Klimov, *Phys. Rev. Lett.* **2004**, *93*, 027401.
[97] K. Matsuda, Y. Kanemitsu, K. Irie, T. Saiki, T. Someya, Y. Miyauchi, S. Maruyama, *Appl. Phys. Lett.* **2005**, *86*, 123116.
[98] K. Balasubramanian, M. Burghard, K. Kern, M. Scolari, A. Mews, *Nano Lett.* **2005**, *5*, 507.
[99] H. Htoon, M. J. O'Connell, S. K. Doorn, V. I. Klimov, *Phys. Rev. Lett.* **2005**, *94*, 127403.
[100] J. U. Lee, *Appl. Phys. Lett.* **2005**, *87*, 073101.
[101] J. Chen, V. Perebeinos, M. Freitag, J. Tsang, Q. Fu, J. Liu, P. Avouris, *Science* **2005**, *310*, 1171.
[102] J. U. Lee, P. J. Codella, M. Pietrzykowski, *Appl. Phys. Lett.* **2007**, *90*, 053103.
[103] L. Cognet, D. A. Tsyboulski, J.-D. R. Rocha, C. D. Doyle, J. M. Tour, R. B. Weisman, *Science* **2007**, *316*, 1465.
[104] A. Högele, C. Galland, M. Winger, A. Imamoğlu, *Phys. Rev. Lett.* **2008**, *100*, 217401.
[105] C. Galland, A. Högele, H. E. Türeci, A. Imamoğlu, *Phys. Rev. Lett.* **2008**, *101*, 067402.
[106] A. Srivastava, H. Htoon, V. I. Klimov, J. Kono, *Phys. Rev. Lett.* **2008**, *101*, 087402.
[107] R. Matsunaga, K. Matsuda, Y. Kanemitsu, *Phys. Rev. Lett.* **2008**, *101*, 147404.
[108] K. Matsuda, T. Inoue, Y. Murakami, S. Maruyama, Y. Kanemitsu, *Phys. Rev. B: Condens. Matter* **2008**, *77*, 033406.
[109] N. M. Gabor, Z. Zhong, K. Bosnick, J. Park, P. L. McEuen, *Science* **2009**, *325*, 1367.
[110] M. Steiner, M. Freitag, V. Perebeinos, A. Naumov, J. P. Small, A. A. Bol, P. Avouris, *Nano Lett.* **2009**, *9*, 3477.
[111] R. Matsunaga, Y. Miyauchi, K. Matsuda, Y. Kanemitsu, *Phys. Rev. B: Condens. Matter* **2009**, *80*, 115436.
[112] M. Freitag, M. Steiner, A. Naumov, J. P. Small, A. A. Bol, V. Perebeinos, P. Avouris, *ACS Nano* **2009**, *3*, 3744.
[113] S. Moritsubo, T. Murai, T. Shimada, Y. Murakami, S. Chiashi, S. Maruyama, Y. K. Kato, *Phys. Rev. Lett.* **2010**, *104*, 247402.
[114] S. Zaric, G. N. Ostojic, J. Kono, J. Shaver, V. C. Moore, M. S. Strano, R. H. Hauge, R. E. Smalley, X. Wei, *Science* **2004**, *304*, 1129.
[115] S. Zaric, G. N. Ostojic, J. Kono, J. Shaver, V. C. Moore, R. H. Hauge, R. E. Smalley, X. Wei, *Nano Lett.* **2004**, *4*, 2219.
[116] M. F. Islam, D. E. Milkie, C. L. Kane, A. G. Yodh, J. M. Kikkawa, *Phys. Rev. Lett.* **2004**, *93*, 037404.
[117] S. Zaric, G. N. Ostojic, J. Shaver, J. Kono, O. Portugall, P. H. Frings, G. L. J. A. Rikken, M. Furis, S. A. Crooker, X. Wei, V. C. Moore, R. H. Hauge, R. E. Smalley, *Phys. Rev. Lett.* **2006**, *96*, 016406.
[118] J. Shaver, J. Kono, O. Portugall, V. Krstic, G. L. J. A. Rikken, Y. Miyauchi, S. Maruyama, V. Perebeinos, *Nano Lett.* **2007**, *7*, 1851.
[119] I. B. Mortimer, R. J. Nicholas, *Phys. Rev. Lett.* **2007**, *98*, 027404.
[120] J. Shaver, J. Kono, *Laser Photonics Rev.* **2007**, *1*, 260.
[121] J. Shaver, S. A. Crooker, J. A. Fagan, E. K. Hobbie, N. Ubrig, O. Portugall, V. Perebeinos, P. Avouris, J. Kono, *Phys. Rev. B: Condens. Matter* **2008**, *78*, 081402.
[122] A. Nish, R. J. Nicholas, C. Faugeras, Z. Bao, M. Potemski, *Phys. Rev. B: Condens. Matter* **2008**, *78*, 245413.
[123] J. Shaver, A. N. G. Parra-Vasquez, S. Hansel, O. Portugall, C. H. Mielke, M. von Ortenberg, R. H. Hauge, M. Pasquali, J. Kono, *ACS Nano* **2009**, *3*, 131.

[124] T. A. Searles, Y. Imanaka, T. Takamasu, H. Ajiki, J. A. Fagan, E. K. Hobbie, J. Kono, *Phys. Rev. Lett.* **2010**, *105*, 017403.
[125] R. J. Chen, N. R. Franklin, J. Kong, J. Cao, T. W. Tombler, Y. Zhang, H. Dai, *Appl. Phys. Lett.* **2001**, *79*, 2258.
[126] A. Fujiwara, Y. Matsuoka, H. Suematsu, N. Ogawa, K. Miyano, H. Kataura, Y. Maniwa, S. Suzuki, Y. Achiba, *Jpn. J. Appl. Phys.* **2001**, *40*, L1229.
[127] M. Shim, G. P. Siddons, *Appl. Phys. Lett.* **2003**, *83*, 3564.
[128] I. A. Levitsky, W. B. Euler, *Appl. Phys. Lett.* **2003**, *83*, 1857.
[129] A. Mohite, S. Chakraborty, P. Gopinath, G. U. Sumanasekera, B. W. Alphenaar, *Appl. Phys. Lett.* **2005**, *86*, 061114.
[130] S. Kazaoui, N. Minami, B. Nalini, Y. Kim, K. Hara, *J. Appl. Phys.* **2005**, *98*, 084314.
[131] X. Qiu, M. Freitag, V. Perebeinos, P. Avouris, *Nano Lett.* **2005**, *5*, 749.
[132] M. E. Itkis, F. Borondics, A. Yu, R. C. Haddon, *Science* **2006**, *312*, 413.
[133] A. Mohite, J.-T. Lin, G. Sumanasekera, B. W. Alphenaar, *Nano Lett.* **2006**, *6*, 1369.
[134] D.-H. Lien, W.-K. Hsu, H.-W. Zan, N.-H. Tai, C.-H. Tsai, *Adv. Mat.* **2006**, *18*, 98.
[135] J.-L. Sun, J. Wei, J.-L. Zhu, D. Xu, X. Liu, H. Sun, D.-H. Wu, N.-L. Wu, *Appl. Phys. Lett.* **2006**, *88*, 131107.
[136] S. Lu, B. Panchapakesan, *Nanotechnology* **2006**, *17*, 1843.
[137] M. Freitag, J. C. Tsang, A. Bol, D. Yuan, J. Liu, P. Avouris, *Nano Lett.* **2007**, *7*, 2037.
[138] J. Wei, Y. Jia, Q. Shu, Z. Gu, K. Wang, D. Zhuang, G. Zhang, Z. Wang, J. Luo, A. Cao, D. Wu, *Nano Lett.* **2007**, *7*, 2317.
[139] A. Behnam, J. L. Johnson, Y. Choi, M. G. Ertosun, A. K. Okyay, P. Kapur, A. Saraswat, C. Krishna, A. Ural, *Appl. Phys. Lett.* **2008**, *92*, 243116.
[140] B. Pradhan, K. Setyowati, H. Liu, D. H. Waldeck, J. Chen, *Nano Lett.* **2008**, *8*, 1142.
[141] C. A. Merchant, N. Markovic, *Appl. Phys. Lett.* **2008**, *92*, 243510.
[142] Y. Jia, J. Wei, K. Wang, A. Cao, Q. Shu, X. Gui, Y. Zhu, D. Zhuang, G. Zhang, B. Ma, L. Wang, W. Liu, Z. Wang, J. Luo, D. Wu, *Adv. Mater.* **2008**, *20*, 4594.
[143] C. A. Merchant, N. Markovic, *Nanotechnology* **2009**, *20*, 175202.
[144] Y. Liu, S. Lu, B. Panchapakesan, *Nanotechnology* **2009**, *20*, 035203.
[145] P. Stokes, L. Liu, J. Zou, L. Zhai, Q. Huo, S. I. Khondaker, *Appl. Phys. Lett.* **2009**, *94*, 042110.
[146] B. K. Sarker, M. Arif, P. Stokes, S. I. Khondaker, *J. Appl. Phys.* **2009**, *106*, 074307.
[147] Z. Li, V. P. Kunets, V. Saini, Y. Xu, E. Dervishi, G. J. Salamo, A. R. Biris, A. S. Biris, *ACS Nano* **2009**, *3*, 1407.
[148] B. C. St-Antoine, D. Ménard, R. Martel, *Nano Lett.* **2009**, *9*, 3503.
[149] P. Castrucci, C. Scilletta, S. D. Gobbo, M. Scarselli, L. Camilli, M. Simeoni, B. Delley, A. Continenza, M. D. Crescenzi, *Nanotechnology* **2011**, *22*, 115701.
[150] L. Xiao, Y. Zhang, Y. Wang, K. Liu, Z. Wang, T. Li, Z. Jiang, J. Shi, L. Liu, Q. Li, Y. Zhao, Z. Feng, S. Fan, K. Jiang, *Nanotechnology* **2011**, *22*, 025502.
[151] M. Omari, N. A. Kouklin, *Appl. Phys. Lett.* **2011**, *98*, 243113.
[152] B. C. St-Antoine, D. Ménard, R. Martel, *Nano Lett.* **2011**, *11*, 609.
[153] B. C. St-Antoine, D. Ménard, R. Martel, *Nano Res.* **2012**, *5*, 73.
[154] M. Passacantando, V. Grossi, S. Santucci, *Appl. Phys. Lett.* **2012**, *100*, 163119.
[155] M. S. Dresselhaus, G. Dresselhaus, R. Saito, *Phys. Rev. B: Condens. Matter* **1992**, *45*, 6234.
[156] J. W. Mintmire, B. I. Dunlap, C. T. White, *Phys. Rev. Lett.* **1992**, *68*, 631.
[157] R. Saito, M. Fujita, G. Dresselhaus, M. S. Dresselhaus, *Phys. Rev. B: Condens. Matter* **1992**, *46*, 1804.
[158] N. Hamada, S. Sawada, A. Oshiyama, *Phys. Rev. Lett.* **1992**, *68*, 1579.
[159] R. Saito, M. Fujita, G. Dresselhaus, M. S. Dresselhaus, *Appl. Phys. Lett.* **1992**, *60*, 2204.
[160] D. H. Robertson, D. W. Brenner, J. W. Mintmire, *Phys. Rev. B: Condens. Matter* **1992**, *45*, 12592.
[161] C. T. White, D. H. Robertson, J. W. Mintmire, *Phys. Rev. B: Condens. Matter* **1993**, *47*, 5485.
[162] R. A. Jishi, M. S. Dresselhaus, G. Dresselhaus, *Phys. Rev. B: Condens. Matter* **1993**, *47*, 16671.
[163] H. Ajiki, T. Ando, *J. Phys. Soc. Jpn.* **1993**, *62*, 1255.
[164] P. S. Davids, L. Wang, A. Saxena, A. R. Bishop, *Phys. Rev. B: Condens. Matter* **1993**, *48*, 17545.
[165] H. Ajiki, T. Ando, *J. Phys. Soc. Jpn.* **1993**, *62*, 2470.
[166] W. Tian, S. Datta, *Phys. Rev. B: Condens. Matter* **1994**, *49*, 5097.
[167] M. F. Lin, K. W. K. Shung, *Phys. Rev. B: Condens. Matter* **1994**, *50*, 17744.
[168] H. Ajiki, T. Ando, *Physica B* **1994**, *201*, 349.
[169] R. Saito, G. Dresselhaus, M. S. Dresselhaus, *Phys. Rev. B: Condens. Matter* **1994**, *50*, 14698.
[170] J. P. Lu, *Phys. Rev. Lett.* **1995**, *74*, 1123.
[171] M. F. Lin, K. W. K. Shung, *Phys. Rev. B: Condens. Matter* **1995**, *52*, 8423.
[172] S. Tasaki, K. Maekawa, T. Yamabe, *Phys. Rev. B: Condens. Matter* **1998**, *57*, 9301.
[173] J. W. Mintmire, C. T. White, *Phys. Rev. Lett.* **1998**, *81*, 2506.
[174] S. Roche, G. Dresselhaus, M. S. Dresselhaus, R. Saito, *Phys. Rev. B: Condens. Matter* **2000**, *62*, 16092.
[175] R. Saito, G. Dresselhaus, M. S. Dresselhaus, *Phys. Rev. B: Condens. Matter* **2000**, *61*, 2981.
[176] L. Yang, J. Han, *Phys. Rev. Lett.* **2000**, *85*, 154.
[177] S. Reich, C. Thomsen, P. Ordejón, *Phys. Rev. B: Condens. Matter* **2002**, *65*, 155411.
[178] A. Grüneis, R. Saito, G. G. Samsonidze, T. Kimura, M. A. Pimenta, A. Jorio, A. G. S. Filho, G. Dresselhaus, M. S. Dresselhaus, *Phys. Rev. B: Condens. Matter* **2003**, *67*, 165402.
[179] I. Miloševič, T. Vukovič, S. Dmitrovič, M. Damnjanovič, *Phys. Rev. B: Condens. Matter* **2003**, *67*, 165418.
[180] H. Sakai, H. Suzuura, T. Ando, *J. Phys. Soc. Jpn.* **2003**, *72*, 1698.
[181] T. Miyake, S. Saito, *Phys. Rev. B: Condens. Matter* **2003**, *68*, 155424.
[182] G. G. Samsonidze, A. Grüneis, R. Saito, A. Jorio, A. G. Souza Filho, G. Dresselhaus, M. S. Dresselhaus, *Phys. Rev. B: Condens. Matter* **2004**, *69*, 205402.
[183] J. Jiang, R. Saito Grüneis, G. Dresselhaus, M. S. Dresselhaus, *Carbon* **2004**, *42*, 3169.
[184] S. V. Goupalov, *Phys. Rev. B: Condens. Matter* **2005**, *72*, 195403.
[185] N. Nemec, G. Cuniberti, *Phys. Rev. B: Condens. Matter* **2006**, *74*, 165411.
[186] M. A. L. Marques, M. d'Avezac, F. Mauri, *Phys. Rev. B: Condens. Matter* **2006**, *73*, 125433.
[187] S. Iijima, *Nature* **1991**, *354*, 56.
[188] "SWCNT assignment chart," Created by Ramesh Sivarajan (© 2003), www.carbonwall.com; Data updated by Erik H. Hároz (2006); see the most updated version at www.ece.rice.edu/~irlabs/research.htm
[189] M. S. Dresselhaus, A. Jorio, M. Hofmann, G. Dresselhaus, R. Saito, *Nano Lett.* **2010**, *10*, 751.
[190] E. H. Hároz, S. M. Bachilo, R. B. Weisman, S. K. Doorn, *Phys. Rev. B: Condens. Matter* **2008**, *77*, 125405.
[191] T. Ando, T. Nakanishi, *J. Phys. Soc. Jpn.* **1998**, *67*, 1704.
[192] C. T. White, T. N. Todorov, *Nature* **1998**, *393*, 240.
[193] M. S. Arnold, S. I. Stupp, M. C. Hersam, *Nano Lett.* **2005**, *5*, 713.
[194] M. S. Arnold, A. A. Green, J. F. Hulvat, S. I. Stupp, M. C. Hersam, *Nature Nanotechnol.* **2006**, *1*, 60.
[195] K. Yanagi, Y. Miyata, H. Kataura, *Appl. Phys. Exp.* **2008**, *1*, 034003.
[196] J. L. Blackburn, T. M. Barnes, M. C. Beard, Y.-H. Kim, R. C. Tenent, T. J. McDonald, B. To, T. J. Coutts, M. J. Heben, *ACS Nano* **2008**, *2*, 1266.

[197] S. Niyogi, C. G. Densmore, S. K. Doorn, *J. Am. Chem. Soc.* **2009**, *131*, 1144.
[198] S. Ghosh, S. M. Bachilo, R. B. Weisman, *Nature Nanotechnol.* **2010**, *5*, 443.
[199] M. Machón, S. Reich, H. Telg, J. Maultzsch, P. Ordejón, C. Thomsen, *Phys. Rev. B: Condens. Matter* **2005**, *71*, 035416.
[200] S. V. Goupalov, *Phys. Rev. B: Condens. Matter* **2005**, *71*, 153404.
[201] J. Jiang, R. Saito, K. Sato, J. S. Park, G. G. Samsonidze, A. Jorio, G. Dresselhaus, M. S. Dresselhaus, *Phys. Rev. B: Condens. Matter* **2007**, *75*, 035405.
[202] E. H. Hároz, J. G. Duque, B. Y. Lu, P. Nikolaev, S. Arepalli, R. H. Hauge, S. K. Doorn, J. Kono, *J. Am. Chem. Soc.* **2012**, *134*, 4461.
[203] E. Prodan, C. Radloff, N. J. Halas, P. Nordlander, *Science* **2003**, *302*, 419.
[204] R. Loudon, *Am. J. Phys.* **1959**, *27*, 649.
[205] R. J. Elliot, R. Loudon, *J. Phys. Chem. Solids* **1959**, *8*, 382.
[206] R. J. Elliot, R. Loudon, *J. Phys. Chem. Solids* **1960**, *15*, 196.
[207] T. Ogawa, T. Takagahara, *Phys. Rev. B: Condens. Matter* **1991**, *43*, 14325.
[208] T. Ogawa, T. Takagahara, *Phys. Rev. B: Condens. Matter* **1991**, *44*, 8138.
[209] M. S. Dresselhaus, G. Dresselhaus, R. Saito, A. Jorio, *Ann. Rev. Phys. Chem.* **2007**, *58*, 719.
[210] T. Ando, *J. Phys. Soc. Jpn.* **1997**, *66*, 1066.
[211] T. Ando, *J. Phys. Soc. Jpn.* **2004**, *73*, 3351.
[212] T. G. Pedersen, *Phys. Rev. B: Condens. Matter* **2003**, *67*, 073401.
[213] C. L. Kane, E. J. Mele, *Phys. Rev. Lett.* **2003**, *90*, 207401.
[214] C. D. Spataru, S. Ismail-Beigi, L. X. Benedict, S. G. Louie, *Phys. Rev. Lett.* **2004**, *92*, 077402.
[215] E. Chang, G. Bussi, A. Ruini, E. Molinari, *Phys. Rev. Lett.* **2004**, *92*, 196401.
[216] T. G. Pederson, *Carbon* **2004**, *42*, 1007.
[217] V. Perebeinos, J. Tersoff, P. Avouris, *Phys. Rev. Lett.* **2004**, *92*, 257402.
[218] C. L. Kane, E. J. Mele, *Phys. Rev. Lett.* **2004**, *93*, 197402.
[219] H. Zhao, S. Mazumdar, *Phys. Rev. Lett.* **2004**, *93*, 157402.
[220] E. Chang, G. Bussi, A. Ruini, E. Molinari, *Phys. Rev. B: Condens. Matter* **2005**, *72*, 195423.
[221] V. Perebeinos, J. Tersoff, P. Avouris, *Nano Lett.* **2005**, *5*, 2495.
[222] C. D. Spataru, S. Ismail-Beigi, R. B. Capaz, S. G. Louie, *Phys. Rev. Lett.* **2005**, *95*, 247402.
[223] E. Chang, D. Prezzi, A. Ruini, E. Molinari, **2006**, cond-mat/0603085.
[224] R. B. Capaz, C. D. Spataru, S. Ismail-Beigi, S. G. Louie, *Phys. Rev. B: Condens. Matter* **2006**, *74*, 121401(R).
[225] J. Jiang, R. Saito, G. G. Samsonidze, A. Jorio, S. G. Chou, G. Dresselhaus, M. S. Dresselhaus, *Phys. Rev. B: Condens. Matter* **2007**, *75*, 035407.
[226] T. Ando, *J. Phys. Soc. Jpn.* **2006**, *75*, 024707.
[227] S. Uryu, T. Ando, *Phys. Rev. B: Condens. Matter* **2006**, *74*, 155411.
[228] S. Uryu, T. Ando, *Phys. Rev. B: Condens. Matter* **2007**, *76*, 115420.
[229] J. Deslippe, C. D. Spataru, D. Prendergast, S. G. Louie, *Nano Lett.* **2007**, *7*, 1626.
[230] S. Kilina, S. Tretiak, S. K. Doorn, Z. Luo, F. Papadimitrakopoulos, A. Piryatinski, A. Saxena, A. R. Bishop, *Proc. Natl. Acad. Sci. USA* **2008**, *105*, 6797.
[231] S. Uryu, T. Ando, *Phys. Rev. B: Condens. Matter* **2008**, *77*, 205407.
[232] P. T. Araujo, A. Jorio, M. S. Dresselhaus, K. Sato, R. Saito, *Phys. Rev. Lett.* **2009**, *103*, 146802.
[233] T. Ando, *J. Phys. Soc. Jpn.* **2010**, *79*, 024706.
[234] A. R. T. Nugraha, R. Saito, K. Sato, P. T. Araujo, A. Jorio, M. S. Dresselhaus, *Appl. Phys. Lett.* **2010**, *97*, 091905.
[235] F. Wang, G. Dukovic, L. E. Brus, T. F. Heinz, *Science* **2005**, *308*, 838.
[236] J. Maultzsch, R. Pomraenke, S. Reich, E. Chang, D. Prezzi, A. Ruini, E. Molinari, M. S. Strano, C. Thomsen, C. Lienau, *Phys. Rev. B: Condens. Matter* **2005**, *72*, 241402.
[237] F. Wang, D. J. Cho, B. Kessler, J. Deslippe, P. J. Schuck, S. G. Louie, A. Zettl, T. F. Heinz, Y. R. Shen, *Phys. Rev. Lett.* **2007**, *99*, 227401.
[238] O. Dubay, G. Kresse, H. Kuzmany, *Phys. Rev. Lett.* **2002**, *88*, 235506.
[239] M. Lazzeri, S. Piscanec, F. Mauri, A. C. Ferrari, J. Robertson, *Phys. Rev. B: Condens. Matter* **2006**, *73*, 155426.
[240] K. Ishikawa, T. Ando, *J. Phys. Soc. Jpn.* **2006**, *75*, 084713.
[241] S. Piscanec, M. Lazzeri, J. Robertson, A. C. Ferrari, F. Mauri, *Phys. Rev. B: Condens. Matter* **2007**, *75*, 035427.
[242] S. D. M. Brown, A. Jorio, P. Corio, M. S. Dresselhaus, G. Dresselhaus, R. Saito, K. Kneipp, *Phys. Rev. B: Condens. Matter* **2001**, *63*, 155414.
[243] K. Kempa, *Phys. Rev. B: Condens. Matter* **2002**, *66*, 195406.
[244] F. Wu, P. Queipo, A. Nasibulin, T. Tsuneta, T. H. Wang, E. Kauppinen, P. J. Hakonen, *Phys. Rev. Lett.* **2007**, *99*, 156803.
[245] K. Sasaki, R. Saito, G. Dresselhaus, M. S. Dresselhaus, H. Farhat, J. Kong, *Phys. Rev. B: Condens. Matter* **2008**, *77*, 245441.
[246] J. S. Park, K. Sasaki, R. Saito, W. Izumida, M. Kalbac, H. Farhat, G. Dresselhaus, M. S. Dresselhaus, *Phys. Rev. B: Condens. Matter* **2009**, *80*, 081402.
[247] K. B. Nordstrom, K. Johnsen, S. J. Allen, A.-P. Jauho, B. Birnir, J. Kono, T. Noda, H. Akiyama, H. Sakaki, *Phys. Rev. Lett.* **1998**, *81*, 457.
[248] A. H. Chin, J. M. Bakker, J. Kono, *Phys. Rev. Lett.* **2000**, *85*, 3293.
[249] A. Srivastava, R. Srivastava, J. Wang, J. Kono, *Phys. Rev. Lett.* **2004**, *93*, 157401.
[250] S. G. Carter, V. Birkedal, C. S. Wang, L. A. Coldren, A. V. Maslov, D. S. Citrin, M. S. Sherwin, *Science* **2005**, *310*, 651.
[251] A. E. Nikolaenko, N. Papasimakis, A. Chipouline, F. De Angelis, E. Di Fabrizio, N. I. Zheludev, *Opt. Exp.* **2012**, *20*, 6068.
[252] G. D. Sanders, C. J. Stanton, J.-H. Kim, K.-J. Yee, Y.-S. Lim, E. H. Hároz, L. G. Booshehri, J. Kono, R. Saito, *Phys. Rev. B: Condens. Matter* **2009**, *79*, 205434.
[253] A. R. T. Nugraha, G. D. Sanders, K. Sato, C. J. Stanton, M. S. Dresselhaus, R. Saito, *Phys. Rev. B: Condens. Matter* **2011**, *84*, 174302.
[254] M. Cardona, *Modulation Spectroscopy*, Academic Press, New York **1969**.
[255] M. A. Meitl, Y. Zhou, A. Gaur, S. Jeon, M. L. Usrey, M. S. Strano, J. A. Rogers, *Nano Lett.* **2004**, *4*, 1643.
[256] Y. Murakami, S. Chiashi, Y. Miyauchi, M. Hu, M. Ogura, T. Okubo, S. Maruyama, *Chem. Phys. Lett.* **2004**, *385*, 298.
[257] K. Hata, D. N. Futaba, K. Mizuno, T. Namai, M. Yumura, S. Iijima, *Science* **2004**, *206*, 1362.
[258] G. Eres, A. A. Kinkhabwala, H. Cui, D. B. Geohegan, A. A. Puretzky, D. H. Lowndes, *J. Phys. Chem. B* **2005**, *109*, 16684.
[259] Y.-Q. Xu, E. Flor, M. J. Kim, B. Hamadani, H. Schmidt, R. E. Smalley, R. H. Hauge, *J. Am. Chem. Soc.* **2006**, *128*, 6560.
[260] S. J. Kang, C. Kocabas, H.-S. Kim, Q. Cao, M. A. Meitl, D.-Y. Khang, J. A. Rogers, *Nano Lett.* **2007**, *7*, 3343.
[261] C. Kocabas, S. Dunham, Q. Cao, K. Cimino, X. Ho, H.-S. Kim, D. Dawson, J. Payne, M. Stuenkel, H. Zhang, T. Banks, M. Feng, S. V. Rotkin, J. A. Rogers, *Nano Lett.* **2009**, *9*, 1937.
[262] F. N. Ishikawa, H.-K. Chang, K. Ryu, P.-c. Chen, A. Badmaev, L. Gomez De Arco, G. Shen, C. Zhou, *ACS Nano* **2009**, *3*, 73.
[263] Y. Lan, Y. Wang, Z. F. Ren, *Adv. Phys.* **2011**, *60*, 553.
[264] Y. Murakami, E. Einarsson, T. Edamura, S. Maruyama, *Phys. Rev. Lett.* **2005**, *94*, 087402.
[265] J. A. Fagan, J. R. Simpson, B. J. Landi, L. J. Richter, I. Mandelbaum, V. Bajpai, D. L. Ho, R. Raffaelle, A. R. Walker, B. J. Bauer, E. K. Hobbie, *Phys. Rev. Lett.* **2007**, *98*, 147402.

[266] C. L. Pint, S. T. Pheasant, K. Coulter, M. Pasquali, H. K. Schmidt, R. H. Hauge, *Nano Lett.* **2008**, *8*, 1879.
[267] C. L. Pint, N. Nicholas, S. T. Pheasant, J. G. Duque, A. N. G. Parra-Vasquez, G. Eres, M. Pasquali, R. H. Hauge, *J. Phys. Chem. C* **2008**, *112*, 14041.
[268] C. L. Pint, Y.-Q. Xu, S. Moghazy, T. Cherukuri, N. T. Alvarez, E. H. Hároz, S. Mahzooni, S. K. Doorn, J. Kono, M. Pasquali, R. H. Hauge, *ACS Nano* **2010**, *4*, 1131.
[269] L. Ren, C. L. Pint, L. G. Booshehri, W. D. Rice, X. Wang, D. J. Hilton, K. Takeya, I. Kawayama, M. Tonouchi, R. H. Hauge, J. Kono, *Nano Lett.* **2009**, *9*, 2610.
[270] L. Ren, C. L. Pint, T. Arikawa, K. Takeya, I. Kawayama, M. Tonouchi, R. H. Hauge, J. Kono, *Nano Lett.* **2012**, *12*, 787.
[271] V. A. Sablikov, B. S. Shchamkhalova, *JETP Lett.* **1997**, *66*, 41.
[272] A. Rosch, N. Andrei, *Phys. Rev. Lett.* **2000**, *85*, 1092.
[273] T. Ando, *J. Phys. Soc. Jpn.* **2002**, *71*, 2505.
[274] P. J. Burke, *IEEE Trans. Nanotechnol.* **2002**, *1*, 129.
[275] M. Pustilnik, M. Khodas, A. Kamenev, L. I. Glazman, *Phys. Rev. Lett.* **2006**, *96*, 196405.
[276] T. Giamarchi, *Quantum Physics in One Dimension*, Oxford University Press, Oxford UK **2004**.
[277] A. Ugawa, A. G. Rinzler, D. B. Tanner, *Phys. Rev. B: Condens. Matter* **1999**, *60*, R11305.
[278] N. Akima, Y. Iwasa, S. Brown, A. M. Barbour, J. Cao, J. L. Musfeldt, H. Matsui, N. Toyota, M. Shiraishi, H. Shimoda, O. Zhou, *Adv. Mater.* **2006**, *18*, 1166.
[279] T. Nakanishi, T. Ando, *J. Phys. Soc. Jpn.* **2009**, *78*, 114708.
[280] F. Borondics, K. Kamarás, M. Nikolou, D. B. Tanner, Z. H. Chen, A. G. Rinzler, *Phys. Rev. B: Condens. Matter* **2006**, *74*, 045431.
[281] H. Nishimura, N. Minami, R. Shimano, *Appl. Phys. Lett.* **2007**, *91*, 011108.
[282] T. Kampfrath, K. von Volkmann, C. M. Aguirre, P. Desjardins, R. Martel, M. Krenz, C. Frischkorn, M. Wolf, L. Perfetti, *Phys. Rev. Lett.* **2008**, *101*, 267403.
[283] G. Y. Slepyan, M. V. Shuba, S. A. Maksimenko, C. Thomsen, A. Lakhtakia, *Phys. Rev. B: Condens. Matter* **2010**, *81*, 205423.
[284] T.-I. Jeon, K.-J. Kim, C. Kang, S.-J. Oh, J.-H. Son, K. H. An, D. J. Bae, Y. H. Lee, *Appl. Phys. Lett.* **2002**, *80*, 3403.
[285] T.-I. Jeon, K.-J. Kim, C. Kang, I. H. Maeng, J.-H. Son, K. H. An, J. Y. Lee, Y. H. Lee, *J. Appl. Phys.* **2004**, *95*, 5736.
[286] J. Kyoung, E.-Y. Jang, M. D. Lima, H.-R. Park, R.-O. Robls, X. Lepro, Y.-H. Kim, R. H. Baughman, D.-S. Kim, *Nano Lett.* **2011**, *11*, 4227.
[287] S. Shoji, H. Suzuki, R. P. Zaccaria, Z. Sekkat, S. Kawata, *Phys. Rev. B: Condens. Matter* **2008**, *77*, 153407.
[288] S. Nanot, A. Cummings, C. L. Pint, A. Ikeuchi, T. Akiho, K. Sueoka, F. Léonard, R. H. Hauge, J. Kono, *unpublished*.